STUDIES ON THE USE OF METAKAOLIN

GEOPOLYMER FOR PRODUCED WATER

TREATMENT

By

YING XU

Bachelor of Engineering in Metallurgical Engineering
University of Science and Technology Beijing
Beijing, China
2015

Submitted to the Faculty of the
Graduate College of the
Oklahoma State University
in partial fulfillment of
the requirements for
the Degree of
MASTER OF SCIENCE
December, 2019

STUDIES ON THE USE OF METAKAOLIN

GEOPOLYMER FOR PRODUCED WATER

TREATMENT

Dissertation Approved:

Dr. Pankaj Sarin
Thesis Advisor

Dr. Raman P. Singh

Dr. Krishnan Ranji Vaidyanathan

ACKNOWLEDGEMENTS

During the last three years as a master's student at the Oklahoma State University, many people have helped me in every aspect which made this dissertation possible. I wish to acknowledge them and express my sincere gratitude.

First and foremost, I would like to show my deepest gratitude to my supervisor, Dr. Sarin, a respectable, responsible and resourceful scholar, who has provided me with invaluable guidance in every stage of this research. Without his enlightening instruction, kindness and patience, I could not have completed my thesis. His keen observation and rigorous scientific approach helped me in overcoming several challenges during this thesis. This education and experience I have gained will most certainly guide me well in my future pursuits.

Knowledge is a vast ocean, and I am only one of the flat boats. I am grateful to the teachers who have given me selfless help in my three years of development, and allowed me get a glimpse of the vastness of this ocean. I would like to extend my thanks to Dr. Lu for all his kindness and help. I would also like to thank Dr. Sarin's research group members who have helped me to develop the fundamental and essential academic competence. I consider myself fortunate have access to some of the top educational resources as a student at the Oklahoma State University which allowed me to complete my study. Last but not least, I'd like to thank my parents and all my friends for their encouragement and support all along.

Name: YING XU

Date of Degree: DECEMBER, 2019

Title of Study: STUDIES ON THE USE OF METAKAOLIN GEOPOLYMER FOR
PRODUCED WATER TREATMENT

Major Field: MATERIALS SCIENCE AND ENGINEERING

Abstract: The looming crisis of drinking water scarcity and rapidly depleting fresh water
resources in the world mandate that we minimize waste and maximize reuse of water. In
the oil and gas (O&G) industry, produced water is a byproduct of O&G extraction, and is
a major cause of wastewater generation. Current produced water handling practices
include reinjection in disposal wells, evaporation in open, with minimal reuse. Recycling
and re-use of produced water is the only solution to minimize the impact of the growing
O&G operations on the future of fresh water supply and the environment. For this
purpose, water treatment and technologies for handling the residual waste are required.

Membrane filtration, which relies on the pore size to separate contaminants is promising
for produced water treatment. Commercial polymeric membranes are not suitable for
produced water treatment due to their substantial maintenance and operation costs.
Ceramic membranes on the other hand promise several advantages, including longer
membrane life, high mechanical strength, superior chemical compatibility, and reduced
process residuals. Unfortunately, the relatively high fabrication cost of ceramic
membranes, which can range from hundreds to thousands of dollars per square meter of
surface area, has restricted their wider application.

This study is the first-ever attempt to develop low-cost ceramic membranes with
controlled porosity using geopolymers for produced water treatment. Membranes were
processed as ceramic composites using geopolymers as the matrix phase and natural
zeolites or biochar as the filler phase. A range of compositions, varying both the
concentration and type of the filler phase, were processed under different conditions. The
membranes were characterized for their microstructure and mechanical properties. The
membrane performance was evaluated for flow rate and ability to remove particulate and
dissolved impurities from produced water. This study confirmed that zeolite is an
excellent choice as a filler phase to develop geopolymer composite membranes for
treating produced water. In addition, the use of pure geopolymer phase to encapsulate
residual waste was also evaluated. This study provides a framework for future studies on
the development of novel geopolymer composites as membranes for water treatment and
for residual waste encapsulation.

TABLE OF CONTENTS

Chapter   Page

LIST OF TABLES

Table   Page

LIST OF FIGURES

Figure   Page

xiv

CHAPTER I

LITERATURE REVIEW

1.1   Produced water

With the increasing awareness about imminent threat of drinking water scarcity and rapidly

depleting fresh water resources in the world, it is very important to minimize waste and maximize

reuse of water in industry applications. In the oil and gas industry water produced as a byproduct

along with oil and gas is referred to as produced water, and is a major cause of waste water

generation. According to global estimates produced water volumes exceed three times the product

volume (Veil, 2011), which translates to about 21 billion barrels per year in the US and 50 billion

barrels per year in the rest of the world over 2009 (Georgie, 2002). Figure 1.1 gives an estimate

of onshore and offshore produced water production since 1990, and forecast in 2015.

Produced water contains both organic and inorganic substances. Some factors such as

geological location of the field, its geological formation, lifetime of its reservoirs, and type of

hydrocarbon product being produced affect the physical and chemical properties of produced

water (Veil et al., 2004). Produced water usually includes the formation water and the injected

fluids from previous treatments. As oil and gas are produced, large quantities of water containing

high levels of total dissolved solids (TDS), hydrocarbons, suspended solids and residual

production chemicals are produced in this process (Lord and LeBas, 2013). The major

compounds of produced water can be
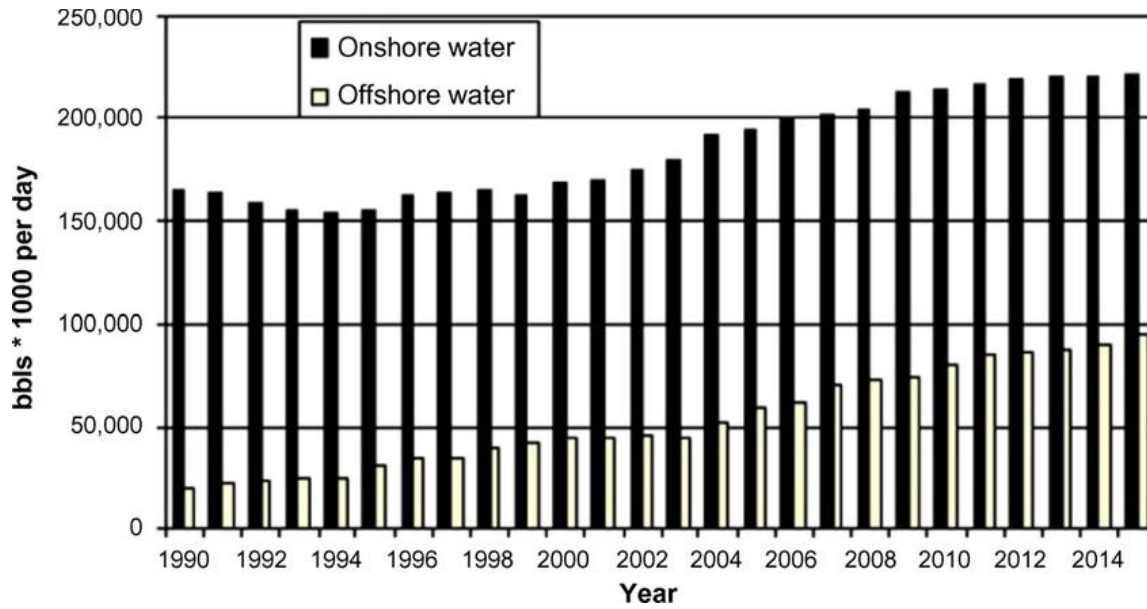
Figure 1.1 Global onshore and offshore water production.(Fakhru'l-Razi et al., 2009)

classified into the following categories:

   a.   Dissolved and dispersed oil compounds

   b.   Dissolved formation minerals

   c.   Production chemical compounds

   d.   Production solids (including formation solids, corrosion and scale products,

        bacteria, waxes, and asphaltenes)

   e.   Dissolved gases (Hansen and Davies, 1994)

     Produced water usually contains elevated concentrations of inorganic (see Table 1.1) and organic constituents. The total dissolved solids (TDS) concentration in produced water can vary between 1,000 mg/L and over 400,000 mg/L. Sodium chloride was found to be most dominant salt found in produced water. Oil and grease, ethyl benzene, benzene, phenols, and toluene are the most common organic contaminants found in produced water. The total oil content in produced water can range from 40 mg/L to 2,000 mg/L.

Table 1.1 Ranges of common inorganic constituents in produced water.(Benko and Drewes, 2008)

Constituent	Units	Low	High	Median
TDS	mg/L	1000	400,000	32,300
Sodium	mg/L	ND	150,000	9,400
Chloride	mg/L	ND	250,000	29,000
Barium	mg/L	ND	850	Unknown
Strontium	mg/L	ND	6,250	Unknown
Sulfate	mg/L	ND	15,000	500
Bicarbonate	mg/L	ND	15,000	400
Calcium	mg/L	ND	74,000	1,500

Note: "unknown" in table signifies information not provided by the source.

1.2   Current practices in produced water handling

Interestingly, discharge of produced water from oil and gas industries into the environment is a common practice(Neff et al., 1992). Current produced water handling practices are dominated by disposal in underground injection control wells, evaporation, with minimal reuse (without treatment). Based on 2015 data from injection wells in Oklahoma, produced water disposal ranged from 0 barrels per day (BPD) to 1,041,173 BPD per county(Oklahoma-PWWG, 2017; OWRB, 2012). Disposal of produced water in underground injection control wells may lead to increased risks of induced seismicity, surface water contamination due to spills during transport, and subsurface fresh water aquifer contamination. In addition, each barrel of produced water that is disposed requires an additional barrel of fresh water as a replacement.

Produced water's toxic substances can cause a lot of harmful effects on the environment. The environmental impact of produced water's salt can also be significant and occur in any area. If discharged in surface water bodies such as rivers or flowing streams, dispersed oil and droplets will float on the surface of the water and the volatile and/or toxic substances will evaporate into the air. These materials increase the biochemical oxygen demand (BOD) of the affected waters

(Stephenson, 1992). Hydrogen sulfide and hydrocarbons are the major toxics compounds to aquatic animals (Neff et al., 1992). Recognizing these possibilities, every region has strict requirements on the quality of discharged sewage. In the North Sea Region, OSPAR regulations set the upper limit for oil content in discharged water at 30 mg/L (Blanchard, 2013).

Currently, the feasibility of reuse of produced water is undermined by the costs of transporting and storing produced water and, particularly, of treating it to a "fit for purpose" level can be cost-prohibitive. Potential risks to health and environment, must be well understood and appropriately managed in order to prevent unintended consequences of reuse. Produced water is complex, and in most cases further research and analysis is needed to better understand and define the "fit for purpose" quality goals for treatment and permitting programs. Environmental considerations beyond direct health or ecosystem impacts include emissions from treatment, managing waste materials from treatment, cumulative ecosystem impacts, or other localized issues.

1.3   Potential for reuse of produced water

The shale oil field requires a large amounts of fresh water in the process of producing oil using hydraulic fracturing. In some cases, each well needs about 4 to 6 million gallons of fresh water. As the restrictions on the availability of underground or surface water sources increases, fresh water will become more and more difficult to obtain. Therefore, increasing produced water reuse holds promise for making available a substantial volume of water that could potentially offset, or supplement, fresh water demands in some areas. Reuse also can be beneficial to oil and gas producers as an alternative to disposal in underground injection control wells, which can be costly, locally unavailable, or subject to volume restrictions. Purposeful intent is also evident in the recent directives to local regulators by some state governments to investigate and consider reuse of produced water for reasons ranging from drought and groundwater depletion to disposal-related induced seismicity.

Water treatment requirements for reusing produced water in hydraulic fracturing are far less demanding than for uses outside the industry. Advances in hydraulic fracturing chemistry have enabled the use of produced water with minimal treatment by addressing only a few specific constituents to create "clean brine." The approach is significantly less costly than more advanced treatment regimes such as those necessary to remove salts.

Treating produced water for reuse in oil and gas industry also brings huge economic benefits. During hydraulic fracturing, a single drilled well is injected up to 4 million gallons of water-based fluid, to create and expand rock fractures, as well as for transport the proppant such as sand or other ceramic materials. 10–70% of the water-based fluid is subsequently pumped back up as produced water. In hydraulic fracturing, the reuse of treated produced water has many advantages such as reduced cost of processing produced water, and also reduced need for fresh water for production.

In some basins, the use of produced water in oil and gas drilling and slickwater-based fracturing treatments has been explored. Typically, these applications use water with low TDS levels. Little work has been done on the use of produced water with high TDS levels (>200,000 ppm) in fracturing fluids designed with linear or crosslinked gel bases. To reuse high-TDS produced water effectively in crosslinked gel-based hydraulic fracturing fluids, the water must first be treated. The goal of the treatment here is to remove only minerals that hinder the development of the crosslinked fluid or that cause scale buildup in the well. Furthermore, if such treatment for reuse can be performed near the production site, recycling and reuse programs will not only have economic benefits, but will also be environmentally beneficial.

In addition, the economic attractiveness of reuse depends on whether the supply of produced water is predictable, whether it can be delivered reliably to the point of use, and how the cost compares to other available sources of water after factoring in the costs of its treatment and transportation as well as the disposal of treatment residuals. The recent emergence of water midstream solutions (coordinating water sourcing for completion operations with produced water

reuse across multiple producing companies) holds promise for smoothing out the peaks and valleys of individual company water demands, reducing transportation and disposal, and reducing demands on infrastructure through shared use. The scale of water midstream could allow reuse to grow steadily, especially in the most active areas in the Permian, Appalachia, West Texas and Oklahoma where disposal options have been or may become limited and disposal costs have been high or are increasing. In addition, several of the top basins are in arid regions with limited availability of sourced water.

1.4   Membrane filtration

Different treatments such as chemical and biological methods have been developed to treat wastewater. The following reasons hamper wider application of these methods:

  a.   High cost of treatment,

  b.   Using toxic chemicals,

  c.   Space for installation,

  d.   Secondary pollution.

As a result, physical, membrane-based separation became the promising technology for the 21st century.

Membranes are thin films of synthetic organic or inorganic materials, which selectively separate a fluid from its components. The membrane pressure-driven process relies on the pore size of the membrane to separate the feed stream components according to their pore sizes (Sonune and Ghate, 2004). Membranes can remove the smallest (<10 µm) and most stable oil droplets. Membranes are used in various applications, from desalination of sea water to treatment of wastewater from the food, leather and oil industry (Cheryan and Rajagopalan, 1998). For all these different applications, appropriate membranes need to be selected. A first classification of membranes can be made based on pore size (Figure 1.2). Microfiltration (MF) membranes, with pores down to 0.1 µm, remove suspended particles, bacteria and some viruses, ultrafiltration (UF)

removes viruses, proteins and colloidal particles and nanofiltration (NF) is selective for

multivalent ions and dissolved compounds. Reverse osmosis (RO) membranes usually allow only

water to pass through. In produced water treatment, the focus is on microfiltration and

ultrafiltration. Reverse osmosis membranes are sometimes used in combination with one of the

former.
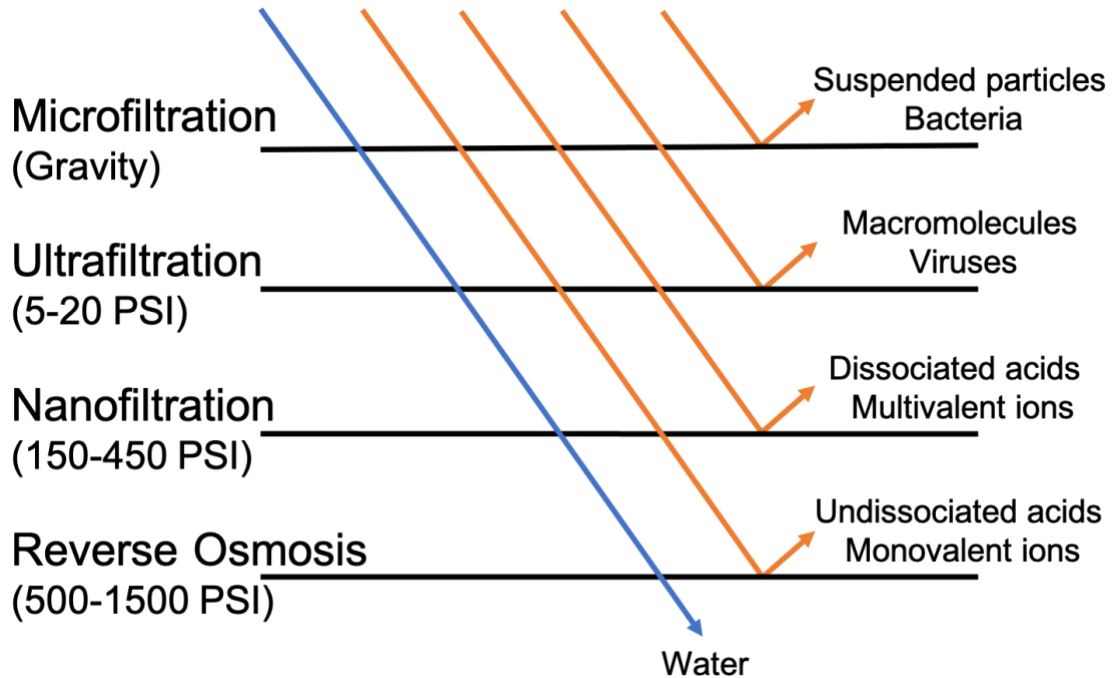
Figure 1.2 Classification of membranes based on pore size.

Membranes can be operated in either dead-end filtration or cross-flow filtration modes. In

dead-end filtration, the retentate concentrates on the membrane, whereas in cross-flow filtration,

the permeate leaves through the pores of the membrane, and the concentrated retentate flows

away over the membrane. Depending on the operating conditions of the membrane, flat-sheet or

hollow fiber membranes can be used. Flat sheet membranes can be rolled into spiral-wound

modules or used in a plate-and-frame setup, which is often used in membrane bed reactor (MBR)

(Judd, 2010). Hollow fiber modules, on the other hand, contain several hundred to thousands of

fibers.

Membrane systems can compete with more complex treatment technologies for treating water with high oil content; low mean particle size, and flow rates greater than 150 m3/h and is, consequently, suitable for medium and large offshore platforms (Ciarapica and Giacchetta, 2003).

UF is one of the most effective methods for oily wastewater treatment, especially for produced water, in comparison with the traditional separation methods because of its high oil removal efficiency, there is no necessity for chemical additives, energy costs are low, and space requirements small (Duxson et al., 2007). In a study, Li *et al.* (Li et al., 2006) studied a tubular UF model equipped with polyvinylidene fluoride membranes modified by inorganic nano-sized alumina particles to treat oilfield-produced water. Nano-sized alumina particles can improve antifouling performance of membranes. Results of their experiments showed that chemical oxygen demand (COD) and total organic carbon (TOC) removal efficiencies of the system were 90% and 98%, respectively, and oil residue was less than 1%.

Bilstad and Espedal (Bilstad and Espedal, 1996) compared MF and UF membranes in pilot trial to treat the North Sea oilfield-produced water. Results showed that UF, but not MF, could meet effluent standards for total hydrocarbons, suspended-sediment (SS), and dissolved constituents. By UF membrane treatment with molecular weight cut-off (MWCO) was between 100,000 and 200,000 Da, total hydrocarbon concentration could be reduced to 2 mg/L from 50 mg/L (96% removal). Benzene, toluene, and xylene (BTX) were reduced by 54%, and some heavy metals like Cu, and Zn were removed to the extent of 95%.

Lee and Frankiewicz (Lee and Frankiewicz, 2005) tested a hydrophilic UF membrane of 0.01μm pore size, in crossflow mode to treat oilfield-produced water. A hydrocyclone was first used to desand and de-oil the wastewater. The hydrocyclone pretreated the raw produced water removing solids and oil content by 73% and 54%, respectively. Oil and gas concentration after UF could be reduced to less than 2 mg/L. The preferred feed-water specification for ideal performance of UF was oil and solids less than 50 and 15 ppm, respectively.

Low-pressure-driven membranes for MF of membrane pore size between 0.1 and 5µm or UF with membrane pore size less than 0.1µm or a combination of MF/UF polymeric or ceramic membranes are suitable for removing oil content of oilfield-produced water. However, ceramic membranes are preferred over delicate polymeric membranes because the former have a better tolerance to high temperature, high oil content, foulants, and strong cleaning agents (Bader, 2007). Ceramic ultra- and NF-membranes are a relatively new class of materials for the treatment of produced water (Bader, 2007).

Chen *et al.* (Chen et al., 1991) tested performance of ceramic crossflow MFs to separate oil, grease, and SS from produced water. Permeate quality of dispersed oil and gas was 5 mg/L and of SS was less than 1 mg/L.

Combined membrane pretreatment and RO technology are effective methods for produced water treatment (Szép and Kohlheb, 2010). Xu *et al.* (Xu et al., 2008) investigated a two-stage laboratory-scale membrane to treat gas field produced water generated from sandstone aquifers as shown in Figure 1.3. They studied ultra-low-pressure RO and NF membranes to meet quality standards for potable and irrigation water, and iodide concentration in brine.
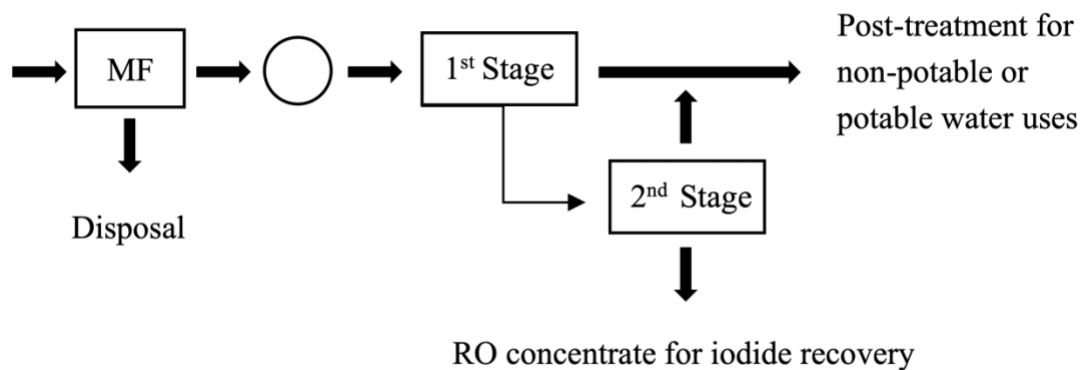
Figure 1.3 Proposed MF and two-stage RO/NF membrane treatment.(Xu et al., 2008)

Membranes can be divided in two groups based on the materials they are made of, namely polymeric or ceramic. Polymeric membranes are used in many separation processes in industry. A wide range of polymers can be used, such as cellulose derivatives, polyvinylidenedifluoride (PVDF), polysulfone (PS), polyether sulfone(PES), polyacrylonitrile (PAN), polytetrafluoroethylene (PTFE) and polyvinylchloride (PVC). These membranes can be tailored to the specific needs of the process they are used in, thus giving the opportunity of selective separation. Selecting a polymeric membrane for a certain task is not a trivial exercise, because the polymer has to have the right affinity and has to withstand the environment of the separation. Polymeric membranes can be either made from pure polymers or from polymers blended with compounds to improve the membrane performance (Lalia et al., 2013). Polymeric membranes can be made both dense and porous, depending on the application. Modifications to the membrane surface can be made to improve the functionality of the membrane (Khulbe et al., 2010).

Ceramic or inorganic membranes, made from materials such as silica, metal oxides or carbon, have superior thermal and chemical stability, and their use in industrial application of oil recovery is an emerging technology (Alpatova et al., 2014; Deriszadeh et al., 2010; Emani et al., 2014). Most ceramic membranes, in contrast to polymeric membranes, are inert to treatment with steam, solvents, strong acids, and have a very long expected lifespan. Although these membranes do suffer from fouling, the flux can be restored by harsh cleaning methods. Unlike polymeric membranes, ceramic membranes do not suffer from swelling in the presence of solvents. Ceramic membranes are used for MF (Barukčić et al., 2014), UF (Murić et al., 2014) and NF (Zeidler et al., 2014). The drawback of ceramic membranes is their high production costs and their weight, although the latter is compensated by a relatively high flux in return. Furthermore, ceramic membranes work mainly on size exclusion, and modifying ceramic membranes for molecular affinity separation is much more difficult than for polymeric membranes.

10

1.5 Disposal of treatment residuals

Treatment of produced water by membrane filtration and/or other methods such as evaporation-condensation, also generates residual waste. Disposal and/or handling of such waste in the form of solids or sludge, is of considerable concern due to its perceived detrimental impact on the environmental. So far, there is no established technology to address this challenge. Reuse of the dried solids to prepare hydraulic fracturing fluids may not be a viable option due to the presence of radioactive content. A potential solution may exist in technologies that encapsulate these solids and prevent their release to the environment.

CHAPTER II

OBJECTIVES

The overall goal of this research was to explore the use of inexpensive ceramic materials for produced water treatment and encapsulation of the resulting waste. Accordingly, the research comprises of two major thrust areas with the following specific objectives:

Objective 1: Evaluate the use of geopolymer based composites to develop inexpensive ceramic membranes for the treatment of produced water.

In this research thrust, the microstructure and chemistry of the ceramic membranes will be engineered. The performance of the developed membranes will be characterized for their ability to reduce the turbidity, total dissolved solids content, and divalent cations concentration in produced water.

Objective 2: Assess the use of geopolymeric materials to encapsulate waste generated from produced water treatment.

For this objective, the waste comprised of both concentrated solution and dried solids obtained by evaporating produced water. The concentrate solution was used to supplement the water required to produce the geoplymeric phase. The solid waste, which is essentially

crystallized water soluble salts present in produced water along with all the inorganic contaminants, was "sealed" inside a geopolymer capsule. The ability of the geopolymeric phase to successfully contain the inorganic waste in both of the above cases was evaluated by leaching studies in water.

CHAPTER III

MATERIALS AND METHODS

3.1 Materials

Inexpensive ceramic membranes were processed as composites using geopolymers as the matrix

phase and naturally abundant zeolites or biochar as the filler phase. Due to geopolymer's

chemical composition, natural zeolites are among the possible raw materials for the production of

geopolymers. Zeolites are crystalline hydrated alumino-silicates, composed of silicon and

aluminium tetrahedra (SiO_4 and AlO_4) and linked by one oxygen atom (Nikolov et al., 2017).

Biochar is commonly used as an adsorbent material for pollutant removal. Using zeolites or

biochar as additives with geopolymeric matrix phase is promising for processing of geopolymer

composite membranes with tailored porosity to enable filtration functionality. Besides physical

properties of the additive phase (see Table 3.1) , the physical properties of the synthesized

composite can be influenced by the processing conditions such as curing conditions, the particle

size (of additives) and concentration and type of the alkaline activator solution.

Table 3.1 Additive material characteristics

Additive	Particle size (mm)	Pore structure	Functional group
Clinoptilolite	> 5 mm	Macroporous	Aluminosilicate
Biochar	0.25-1.25	Macroporous	Carboxylate

3.1.1 Geopolymers

The reaction of a solid aluminosilicate with a highly concentrated aqueous alkali hydroxide or silicate solution produces a synthetic alkali aluminosilicate material generically called a 'geopolymer', after Davidovits (Zeidler et al., 2014), but probably more appropriately referred to as an example of what is more broadly termed an 'inorganic polymer' (Davidovits, 1989). These materials can provide comparable performance to traditional cementitious binders in a range of applications, but with the added advantage of significantly reduced Greenhouse emissions (Gartner, 2004).

'Geopolymer' is generically used to describe the amorphous to crystalline reaction products from synthesis of alkali aluminosilicates from reaction with alkali hydroxide/alkali silicate solution, geopolymeric gels and composites are also commonly referred to as 'low-temperature aluminosilicate glass' (Rahier et al., 1996). 'alkali-activated cement' (Palomo and López dela Fuente, 2003), 'geocement' (Krivenko and Kovalchuk, 2007), 'alkali-bonded ceramic' (Sonune and Ghate, 2004), 'inorganic polymer concrete' (Sofi et al., 2007), and 'hydroceramic' (Bao et al., 2005). Despite this variety of nomenclature, these terms all describe materials synthesized utilizing the same chemistry, which can be described as a complex system of coupled alkali mediated dissolution and precipitation reactions in an aqueous reaction substrate.

Figure 3.1 presents a highly simplified reaction mechanism for geopolymerization. Dissolution of the solid aluminosilicate source by alkaline hydrolysis (consuming water) produces aluminate and silicate species. Once in solution the species released by dissolution are incorporated into the aqueous phase, which may already contain silicate present in the activating solution. A complex mixture of silicate, aluminate and aluminosilicate species is thereby formed (Swaddle, 2001; Swaddle et al., 1994). Dissolution of amorphous aluminosilicates is rapid at high pH, and this quickly creates a supersaturated aluminosilicate solution. In concentrated solutions

this results in the formation of a gel, as the oligomers in the aqueous phase form large networks

by condensation. This process releases the water that was nominally consumed during

dissolution. As such, water plays the role of a reaction
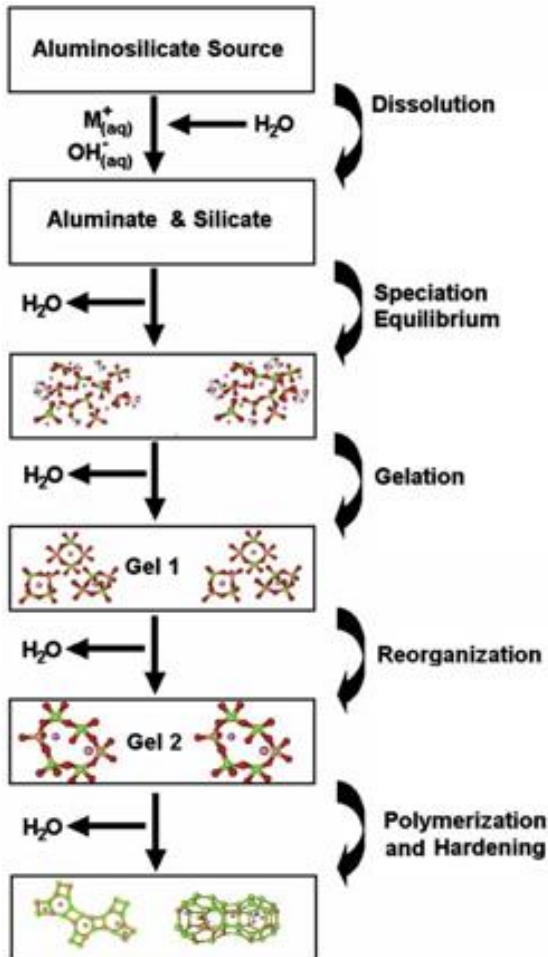
Figure 3.1 Conceptual model for geopolymerization. (Duxson et al., 2007)

medium, but resides within pores in the gel. This type of gel structure is commonly referred to as

bi-phasic, with the aluminosilicate binder and water forming the two phases. The system

continues to rearrange and reorganize, as the connectivity of the gel network increases, resulting

in the three-dimensional aluminosilicate network commonly attributed to geopolymers (Figure

3.2) (Duxson et al., 2007; Fernández-Jiménez et al., 2006). Figure 3.2 describes the activation

reaction as an outcome of two successive and controlling stages. Nucleation, or the dissolution of

16

the aluminosilicate material and formation of polymeric species, is highly dependent on

thermodynamic and kinetic parameters and encompasses the two first steps. Growth is the stage

during which the nuclei reach a critical size and crystals begin to develop. These processes of

structural reorganization determine the microstructure and pore distribution of the material, which

are critical in determining many physical properties (Fernández-Jiménez et al., 2006; van

Jaarsveld and Van Deventer, 1999). Their microstructure consists of chains or networks of

inorganic molecules linked by covalent bounds (Davidovits, 2008). These molecules are

composed from one silicon or aluminium atom connected by four oxygen atoms forming

tetrahedrons, which are connected to each other in a three-dimensional network sharing one

common oxygen atom.
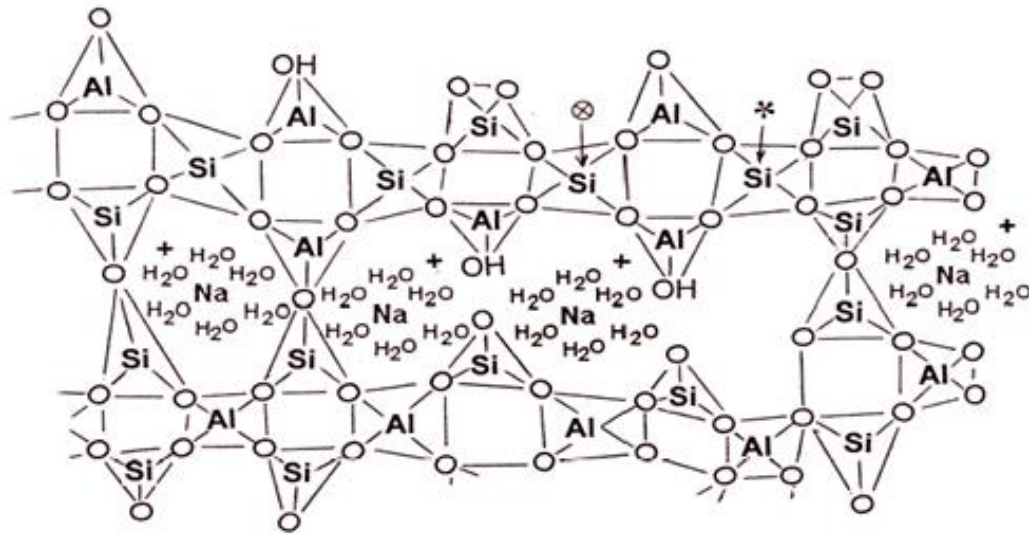
Figure 3.2 Theoretical structure of sodium based geopolymer. (Škvára, 2007)

The settling and hardening reactions take place at room temperature, but sometimes

slightly elevated curing temperatures (up to 80°C) are used to enhance some properties. Hardened

products may possess mechanical properties comparable to ordinary Portland cement concrete

(OPC) or even better. Geopolymers exhibit good thermal and fire resistance of up to 1300 °C (He

et al., 2010) excellent sulphate resistance (Bhutta et al., 2013; Bhutta et al., 2014), high acid

17

resistance (Bakharev, 2005; Thokchom et al., 2009) and satisfactory adhesion to iron, steel and concrete (Castel and Foster, 2015; Temuujin et al., 2009).
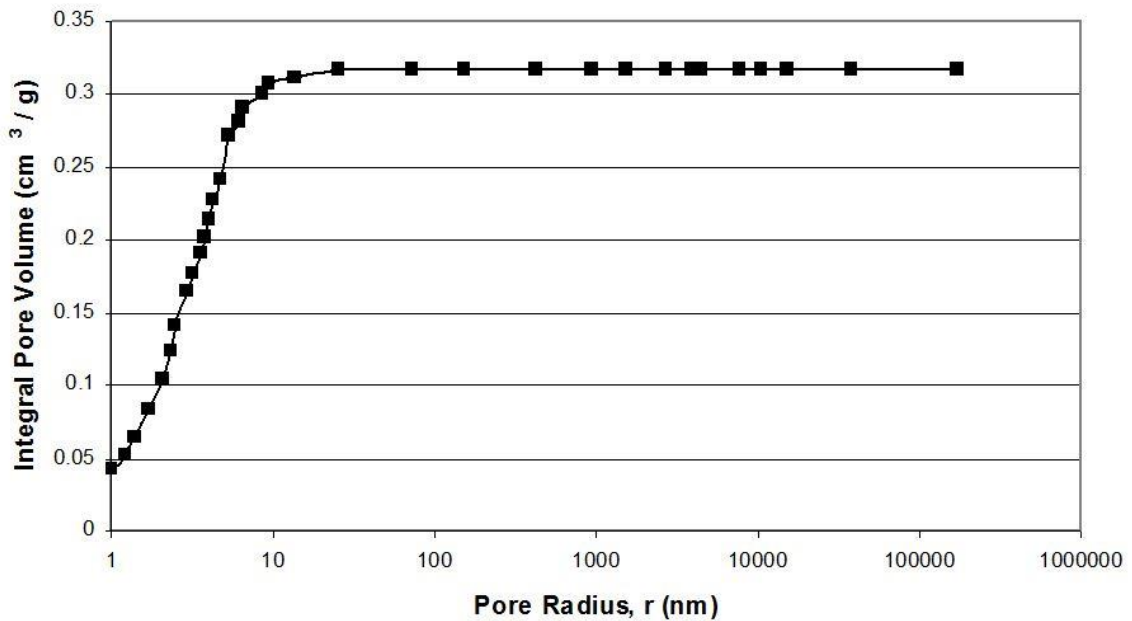
Figure 3.3 Integral pore volume vs pore radius shows 1-10 nm pores. (Duxson et al., 2005)

Depending on the raw material selection and processing conditions, geopolymers can exhibit a wide variety of properties and characteristics, including high compressive strength, low shrinkage, fast or slow setting, acid resistance, fire resistance and low thermal conductivity. Porosimetry analysis (see Figure 3.3) had confirmed that the average pore size in geopolymers is less than four nanometers and that 95% of the internal surface area is present in pores of diameter less than ten nanometers. Geopolymers are, however, impermeable materials, with a measured permeability value of 10_{-9} cm/s (Mallicoat et al., 2005). Accordingly, geopolymers are used in thermal insulation material, polishing-resistant material and building material.

Geopolymer samples are commonly prepared by using commercially available metakaolin and reactive ingredients as raw materials. The reactive ingredients include a solution

18

of water glass (prepared by dissolving potassium hydroxide (KOH) flakes in distilled water) and silica fume. Based on these raw materials, the slurry with 33.1 wt% metakaolin content results in the following theoretical oxide molar ratios: $SiO_2 /Al_2O_3 = 4$, $K_2O/ SiO_2 = 0.25$ and $H_2O/K_2O = 11/13$.

3.1.2 Natural zeolites - Clinoptilolite

Zeolites are microporous, aluminosilicate minerals commonly used as commercial adsorbents and catalysts (Korkuna et al., 2006). The term zeolite was originally coined in 1756 by Swedish mineralogist Axel Fredrik Cronstedt, who observed that rapidly heating the material, believed to have been stilbite, produced large amounts of steam from water that had been adsorbed by the material. Based on this, he called the material zeolite (Cronstedt et al., 1993).
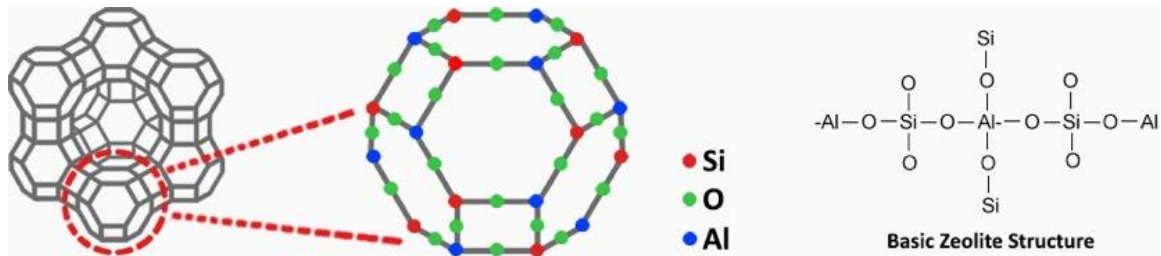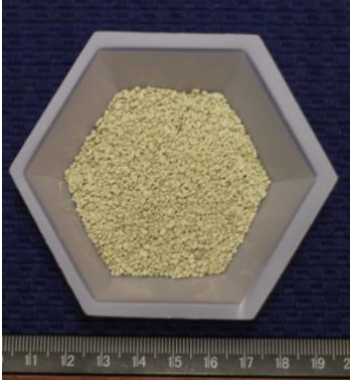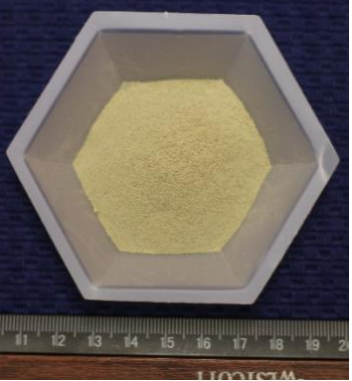
Figure 3.4 Crystal structure of zeolite. (https://www.rotamining.com/what-is-zeolite/)

Zeolites have a porous structure that can accommodate a wide variety of cations, such as Na_+, K_+, Ca_{2+}, Mg_{2+} and others. These positive ions are rather loosely held and can readily be exchanged for others in a contact solution. Some of the more common mineral zeolites are analcime, chabazite, clinoptilolite, heulandite, natrolite, phillipsite, and stilbite. An example of the mineral formula of a zeolite is: $Na_2Al_2Si_3O_{10} \cdot 2H_2O$, the formula for natrolite. These cation exchanged zeolites possess different acidity and catalyze several acid catalysis (Marakatti, 2015a, b).

For this research commercially available clinoptilolite zeolite (Clinoptilolite Zeolite 97% + Purity, KMI Zeolite, Amargosa Valley, NV) with the chemical formula $Na_6[Al_6Si_{30}O_{72}]24H_2O$

was used. Three different sizes of clinoptilolite were used, and their properties, as provided from

the vendor, are included in Table 3.2.

Table 3.2 Physical appearance and properties of the three different types of Clinoptilolite Zeolite (from KMI Zeolite) that were used in this research.

Coarse	**Medium**	**Fine**
Mesh Size: 20/30-	Mesh Size: 14 x 30	Mesh Size: 4 x 8

Parameters	**Values**
Chemical Formula	$Na_6[Al_6Si_{30}O_{72}]24H_2O$
Clinoptilolite Content	97%+
Form	Granules and powders
Pore Diameter	4.0 - 7.0 angstroms
Specific Gravity	1.89
Specific Surface Area	40 m_2/g
Bulk Density	45 - 54 lbs/ft$_3$
pH stability	3.0 - 10.00
Hardness	4.0 – 5.0 Mohs
Swelling Index	Nil
Cation Exchange	1.6 – 2.0 meg/g

Table 3.3 Chemical analysis of commercial Clinoptilolite Zeolite (from KMI Zeolite)

SiO_2	Al_2O_3	Fe_2O_3	CaO	MgO	Na_2O	K_2O	MnO	TiO_2
66.7%	11.48%	0.9%	1.33%	0.27%	3.96%	3.42%	0.025%	0.13%

The chemical composition of the zeolites as provided from the vendor is included in Table 3.3 as oxide phases. The composition analysis was also confirmed by X-Ray Fluorescence (XRF), and the results are included in Table 3.4. Details on the XRF measurements and analysis are included in section 3.3.6.

Table 3.4 XRF analysis of the Clinoptilolite Zeolite (from KMI Zeolite)

Elements	Content (ppm)
Si	587000
Ca	113000
Al	101000
K	95600
Fe	42900
Na	31400
Mg	8240
P	5210
Ti	4570
Sr	2460
Mn	2200
Ba	1890
S	1390
Rb	805
Re	495
Cl	494
Zr	470
As	167
Nb	94
Ga	87
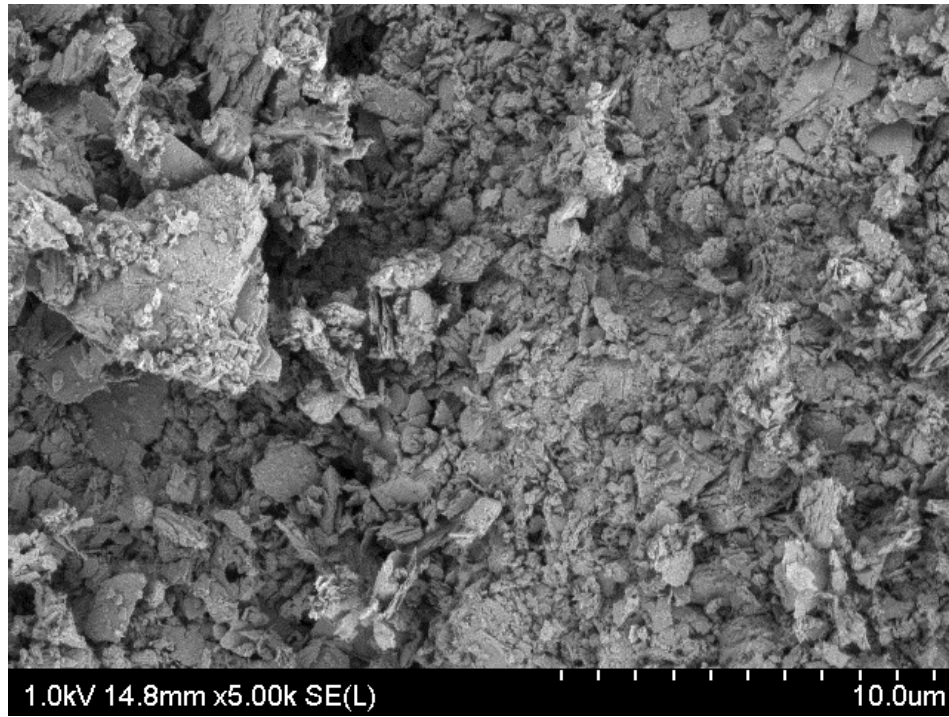
(a)
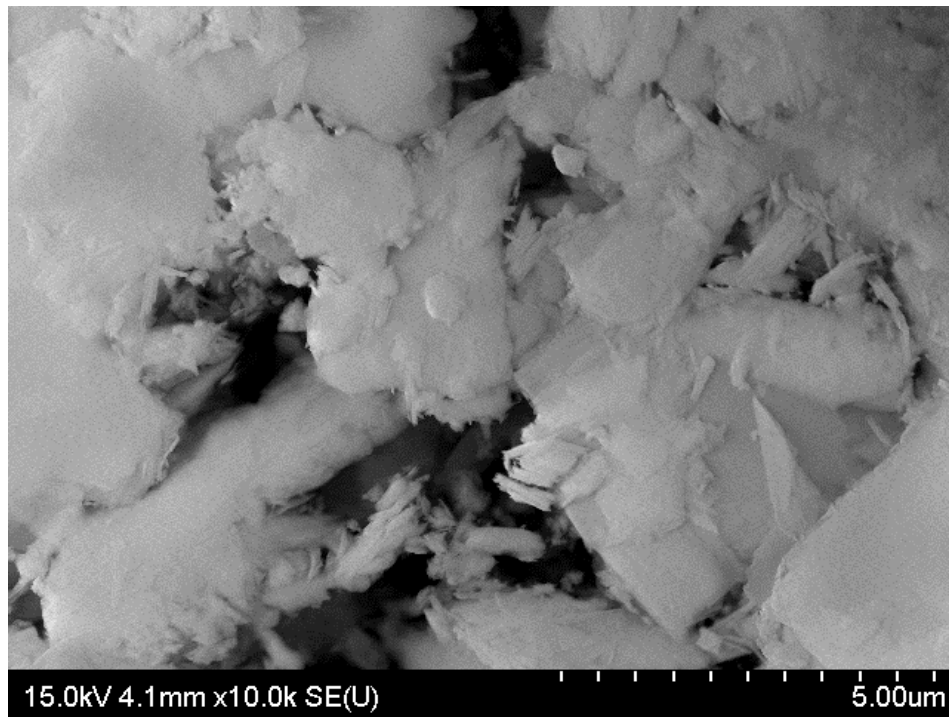
(b)

Figure 3.5 SEM images of Clinoptilolite powder (a) fine grade and (b) medium grade at low magnification.
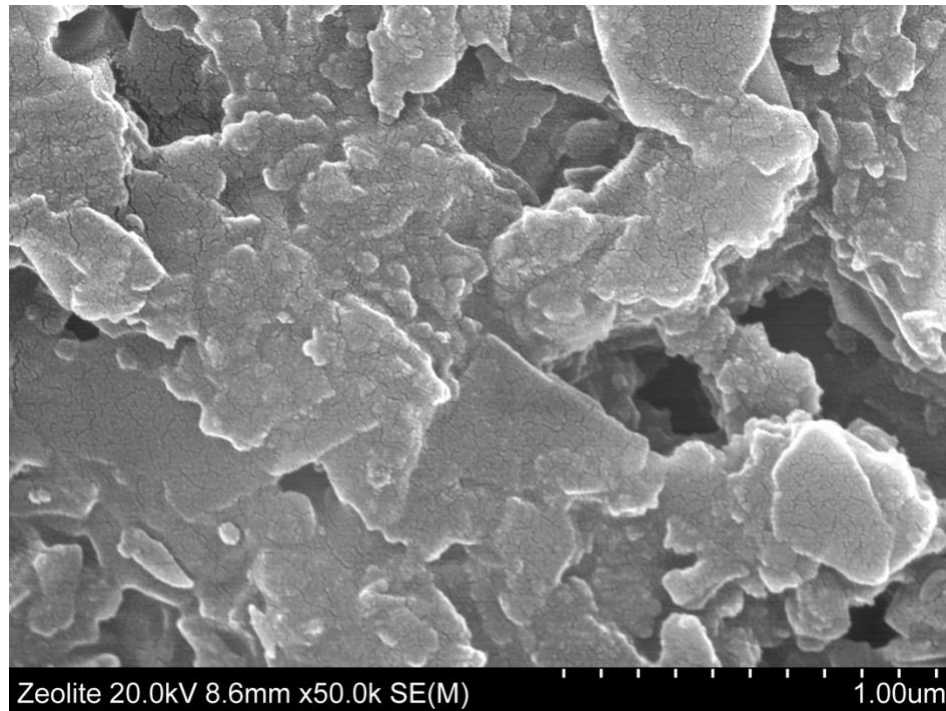
Figure 3.6 SEM image of Coarse Clinoptilolite powder at high magnification.

In addition to the compositional analysis, a thorough examination of the morphology of the clinoptilolite was conducted using scanning electron microscopy (SEM). Details of the SEM sample preparation and analysis are included in section 3.3.5. Low magnification images of the fine and medium grade clinoptilolite powders are shown in Figure 3.5 (a) and (b) respectively. The powders showed a range of sizes and shapes, both large grains as well as acicular grains. For the purpose of high magnification studies using SEM, coarse clinoptilolite particles were first embedded in epoxy, polished to < 1 μm surface finish, and finally coated with gold (Au). Figure 3.6 shows the SEM micrograph at 50,000 X magnification. Large particles were comprised of several smaller grains < 1μm in size. This observation is consistent with most naturally occurring zeolites.

3.1.3 Biochar

Biochar is charcoal used as a soil amendment. Biochar is a stable solid, rich in carbon, and can endure in soil for thousands of years (Glaser et al., 2002). Like most charcoal, biochar is made from biomass via pyrolysis.

Biochar is a high-carbon, fine-grained residue that today is produced through modern pyrolysis processes; it is the direct thermal decomposition of biomass in the absence of oxygen (preventing combustion), which produces a mixture of solids (the biochar proper), liquid (bio-oil), and gas (syngas) products. The specific yield from the pyrolysis is dependent on process condition, such as temperature, residence time and heating rate (Tripathi et al., 2016). These parameters can be optimized to produce either energy or biochar (Gaunt and Lehmann, 2008). Temperatures of 400–500 °C (673–773 K) produce more char, while temperatures above 700 °C (973 K) favor the yield of liquid and gas fuel components (Winsley, 2007). Pyrolysis occurs more quickly at the higher temperatures, typically requiring seconds instead of hours. The increasing heating rate will also lead to a decrease of pyrolysis biochar yield, while the temperature is in the range of 350–600 °C (623–873 K) (Aysu and Küçük, 2014). Typical yields are 60% bio-oil, 20% biochar, and 20% syngas. By comparison, slow pyrolysis can produce substantially more char ($\approx$ 35%) (Winsley, 2007); it is this which contributes to the observed soil fertility of terra preta. Once initialized, both processes produce net energy. For typical inputs, the energy required to run a "fast" pyrolyzer is approximately 15% of the energy that it outputs (Gaunt and Lehmann, 2008). Modern pyrolysis plants can use the syngas created by the pyrolysis process and output 3–9 times the amount of energy required to run.

Besides pyrolysis, torrefaction and hydrothermal carbonization process can also thermally decompose biomass to the solid material. However, these products cannot be strictly defined as biochar. The carbon product from the torrefaction process still contains some volatile organic components, thus its properties are between that of biomass feedstock and biochar

(Kambo and Dutta, 2015). Furthermore, even the hydrothermal carbonization could produce a carbon-rich solid product, the hydrothermal carbonization is evidently different from the conventional thermal conversion process (Bridgwater et al., 2002). Therefore, the solid product from hydrothermal carbonization is defined as "hydrochar" rather than "biochar".

For this research biochar prepared from almond shells was used. The composition analysis was also confirmed by X-Ray Fluorescence (XRF), and the results are included in Table 3.5. Details on the XRF measurements and analysis are included in section 3.3.6.

Table 3.5 XRF analysis of the biochar used in this research .

Elements	Content (ppm)
Si	587000
Ca	113000
Al	101000
K	95600
Fe	42900
Na	31400
Mg	8240
P	5210
Ti	4570
Sr	2460
Mn	2200
Ba	1890
S	1390
Rb	805
Re	495
Cl	494
Zr	470
As	167
Nb	94
Ga	87

powder 25.0kV 6.0mm x5.00k SE(M)   10.0um

(a)

powder 25.0kV 6.0mm x10.0k SE(M)   5.00um

(b)

Figure 3.7 SEM images of biochar powder at (a) 5,000 X and (b) 10,000 X magnification.
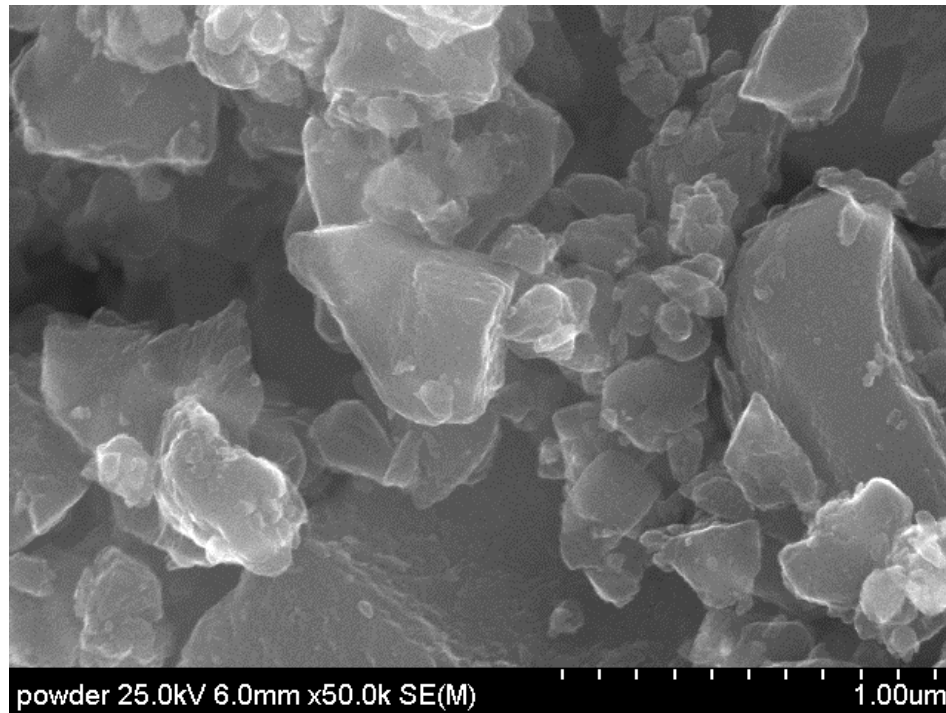
Figure 3.8 SEM image of biochar powder at high magnification.

A thorough examination of the morphology of the biochar was conducted using SEM. Low magnification images of the biochar powders are shown in Figure 3.6 (a) and (b). The powders showed a range of sizes but were largely prismatic. This was further confirmed through high magnification studies using SEM, Figure 3.8. Particles were usually single granular with smooth surfaces, which is consistent with most reports in the literature.

3.2 Methods – Synthesis and Processing

3.2.1 Geopolymer synthesis

Geopolymer samples were prepared by mechanical mixing of stoichiometric amounts of metakaolin ($Al_2O_3.2SiO_2$) and the reactive alkali solution, a solution of potassium hydroxide (KOH), silica fume (SiO_2) and water, to give $K_2O/Al_2O_3=1$. Figure 3.9 shows a schematic diagram of the process used for geopolymer processing. The Thinky mixer (ARE-310 Thinky,
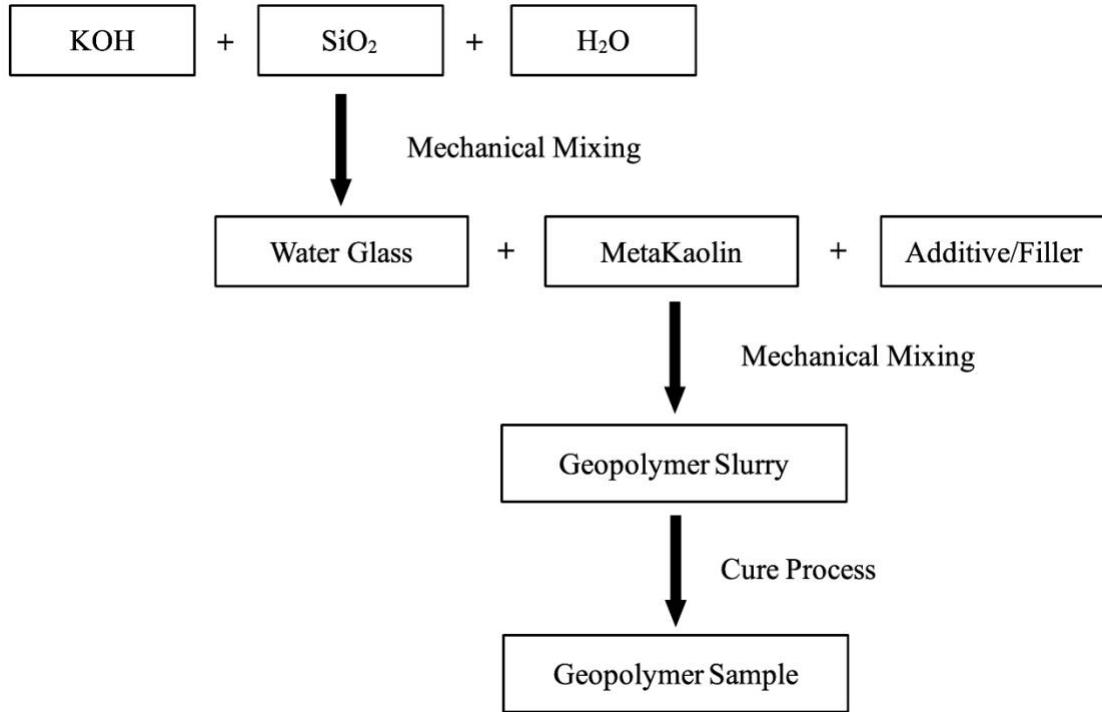
Figure 3.9 Schematic showing the various steps involved in processing geopolymers and geopolymer composites.

CA, USA), shown in Figure 3.10, was used for this purpose and mixing was conducted for 10 min at 1500 rpm, followed by defoaming for 5 min at 2000 rpm. All mixing was done at room temperature, and resulted in the formation of a homogenous slurry. Once the pure geopolymer slurry was successfully prepared, additives were added (if desired) to the slurry and mixed in the Thinky mixer for additional 5 minutes at 1500 rpm. After mechanical mixing of the additive, the slurry was vibrated for further 5 min (using Syntron Paper Jogger, J-1 Flat Deck; D.L. Williams Company, Bluefield, VA, USA) to remove entrained air before being transferred to plastic moulds and sealed from the atmosphere. Samples were cured in Controlled Temperature and Humidity Chamber (TestEquity 123H Controlled Temperature and Humidity Chamber, TestEquity, CA, USA) in two steps (Figure 3.11). In the first step, the sealed container was kept overnight at 40 °C, to prevent cracking due to an abrupt loss of water and promote the geopolymerization reaction. Subsequently, the temperature and conditions were changed to 60 °C

Figure 3.10 ARE-310 Thinky mixer used for geopolymer composite processing in this research.

Figure 3.11 Temperature and humidity control chamber used for geopolymer composite processing.

(a)	(b)	(c)
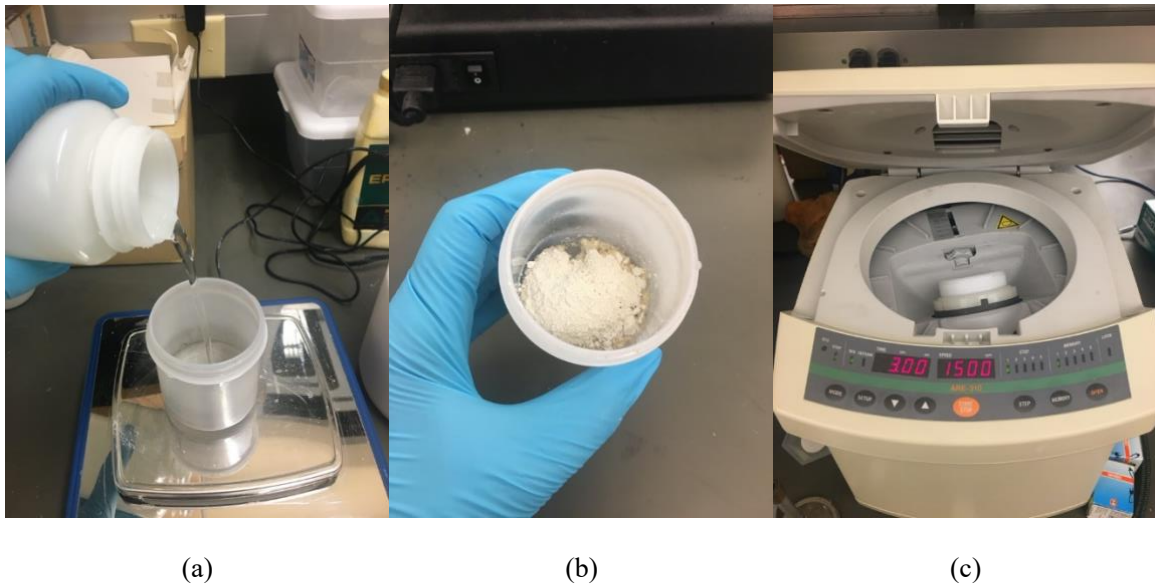
Figure 3.12 Process of making geopolymers (a) Weigh the weight of the waterglass. (b) Add metakaolin in the waterglass. (c) Mechanical mixing the geopolymer slurry.

and 80% relative humidity and maintained for 5 days, to consolidate the structure (Bai et al., 2017). Figure 3.12 shows the actual process of making geopolymers.

3.3 Methods - Characterization

3.3.1 pH

Produced water and filtered water samples were characterized with pH meter (SevenCompact pH meter S220, Mettler-Toledo, LLC, Columbus, OH) to verify the water quality before and after filtration. The instrument was calibrated regularly, as per the instrument manual using standard buffer solutions.

Figure 3.13 SevenCompact pH meter S220 was used for pH measurement of water samples.

3.3.2 TDS/Conductivity

Total dissolved solids (TDS) is a measure of the dissolved combined content of all inorganic and organic substances present in a liquid in molecular, ionized, or micro-granular (colloidal sol) suspended form. Generally, the operational definition is that the solids must be small enough to survive filtration through a filter with 2-micrometer (nominal size, or smaller) pores.

The two principal methods of measuring total dissolved solids are gravimetric analysis and conductivity (EPA Method 160.1). Gravimetric methods are the most accurate and involve evaporating the liquid solvent and measuring the mass of residues left. This method is generally the best, although
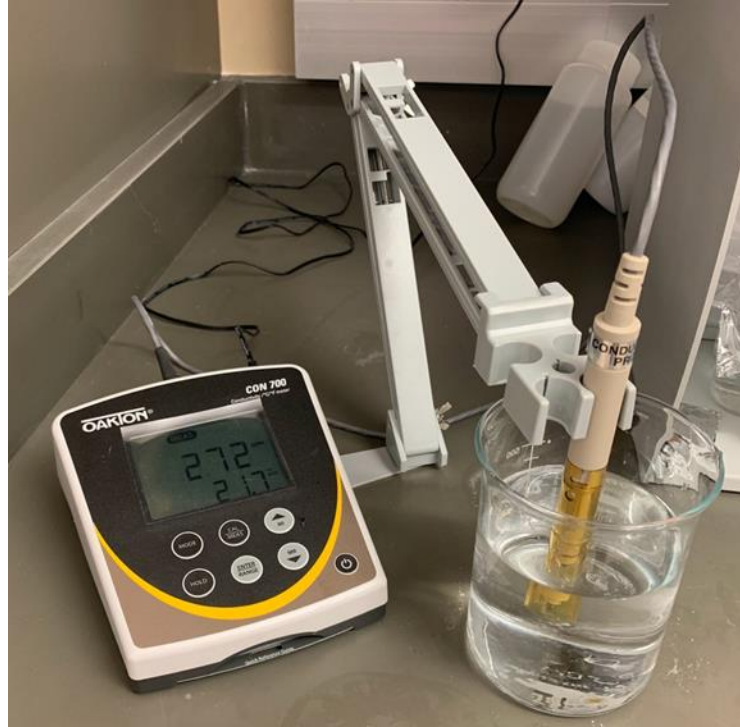
Figure 3.14 The Oakton Con 700 Total Dissolved Solid (TDS) meter (Oakton Instruments, Vernon Hills, IL).

it is time-consuming. If inorganic salts comprise the great majority of TDS, gravimetric methods are appropriate.

Electrical conductivity of water is directly related to the concentration of dissolved ionized solids in the water. Ions from the dissolved solids in water create the ability for that water to conduct an electric current, which can be measured using a conventional conductivity meter or TDS meter. When correlated with laboratory TDS measurements, conductivity provides an approximate value for the TDS concentration, usually to within ten-percent accuracy The relationship of TDS and specific conductance of groundwater can be approximated by the following equation:

$$TDS = k_e EC$$

where TDS is expressed in mg/L and EC is the electrical conductivity in microsiemens percentimeter at 25 °C. The correlation factor k_e varies between 0.55 and 0.8.

For this study the Oakton Con 700 Total Dissolved Solid (TDS) meter (Oakton

Instruments, Vernon Hills, IL) was used. The instrument was calibrated following the procedures

outlined by the instrument manufacturer.

3.3.3 Turbidity

Turbidity is the cloudiness or haziness of a fluid caused by large numbers of individual particles

that are generally invisible to the naked eye, similar to smoke in air. The measurement of

turbidity is a key test of water quality. Fluids can contain suspended solid matter consisting of

particles of many different sizes. While some suspended material will be large enough and heavy

enough to settle rapidly to the bottom of the container if a liquid sample is left to stand (the

settable solids), very small particles will settle only very slowly or not at all if the sample is

regularly agitated or the particles are colloidal. These small solid particles cause the liquid to

appear turbid.

Figure 3.15 The LaMotte 1970-EPA Model 2020we Portable Turbidity Meter (LaMotte Company, Chestertown, MD).

The most widely used measurement unit for turbidity is the Formazin Turbidity Unit

(FTU). ISO refers to its units as FNU (Formazin Nephelometric Units). ISO 7027 provides the

method in water quality for the determination of turbidity. It is used to determine the

concentration of suspended particles in a sample of water by measuring the incident light

scattered at right angles from the sample. The scattered light is captured by a photodiode, which

produces an electronic signal that is converted to a turbidity. Open source hardware has been

developed following the ISO 7027 method to measure turbidity reliably using an Arduino

microcontroller and inexpensive LEDs.

For this study the LaMotte 1970-EPA Model 2020we Portable Turbidity Meter (LaMotte

Company, Chestertown, MD) shown in Figure 3.15 was used. The instrument was calibrated

following the instrument manual provided by the manufacturer.

3.3.4 Optical microscopy

The microstructure of the processed geopolymer composite membranes was studied using an

optical microscope. Digital images were acquired using the Carl Zeiss' AxioLab A1 Modular,

upright Optical Microscope for Materials Science (Carl Zeiss Microscopy, LLC, White Plains,

NY) with 5X, 20X and 100X magnifying lenses. Optical microscope was used to observe the

porosity and filler phase distribution on the surface of the geopolymer and geopolymer composite

Figure 3.16 The Carl Zeiss' AxioLab A1 Modular, upright Optical Microscope for Materials
Science (Carl Zeiss Microscopy, LLC, White Plains, NY) that was used for this study. .

membrane samples. The samples used for these measurements were thin membrane discs cut using the slow action diamond saw. The sample surface was not polished, and represented the surface of the membrane after it was cut using the diamond saw. The magnification of the optical microscope was calibrated using a standard, and scale bars were included on each image to denote the length scale of the observed features.

3.3.5 SEM

A Hitachi S-4800 field emission scanning electron microscope (FE-SEM) coupled with an Oxford Instruments (Tubney Woods, Abingdon, Oxon, UK) energy dispersive spectroscopy (EDS) silicon drift detector was used to characterize the microstructure and determine the elemental composition and distribution of the samples (see Figure 3.17). These included powder/granular samples of the biochar and the clinoptilolite zeolite, and solid samples of the The solid membranes samples included membrane samples before and after they had been tested for their filtration performance.

The post-test membrane samples were small pieces of the composite membrane with particles retained on their surface when produced water was filtered through them. The top surface of these samples (where separation occurs) was coated with a thin layer of gold (Au) using Edwards Sputter Coater S150B (Edwards Vacuum LLC, Albany, NY), shown in Figure 3.18, for 30 s to prevent any charging of the surface during SEM studies. Elemental distribution on the surface was carefully examined to observe the residual particles that were retained by the filter. Elemental maps were acquired using an accelerating voltage of 30 keV at a working distance of 15mm. Samples for SEM were prepared by gold spray or carbon spray, this did not produce fully dense samples but was satisfactory for the intended analysis.

The pre-test or virgin filter samples were first vacuum impregnated (using Citovac, Struers Inc., Cleveland, OH) with epoxy (Epothin, Buehler, Lake Bluff, IL), and polished to
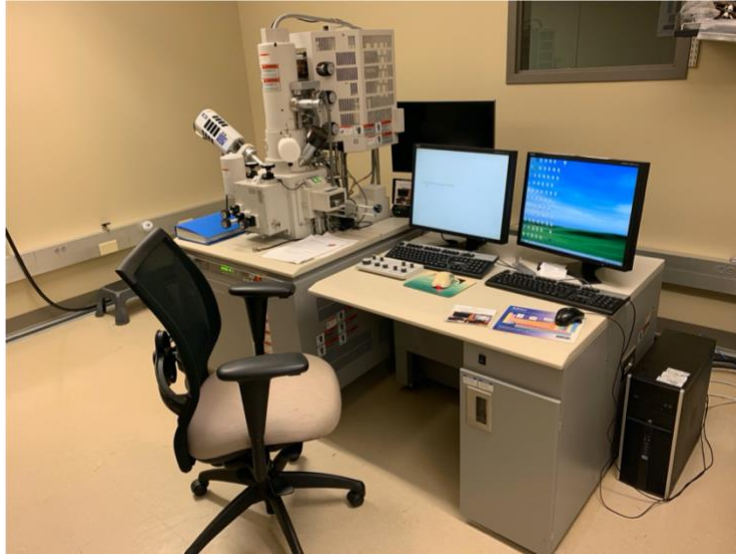
Figure 3.17 Hitachi S-4800 field emission scanning electron microscope (FE-SEM) coupled with an Oxford Instruments (Tubney Woods, Abingdon, Oxon, UK) energy dispersive spectroscopy (EDS) silicon drift detector that was used for this study. .

Figure 3.18 The Edwards Sputter Coater S150B (Edwards Vacuum LLC, Albany, NY) that was used for this study to coat Au on powder/granular and solid membrane samples. .

< 1μm surface finish using Struers LaboPol-35 Polishing/Grinding System, (Struers Inc.,

Cleveland, OH) and SiC polishing papers of different grades. Subsequently, these samples were

cleaned with DI water, dried overnight in vacuum oven (VWR Symphony, VWR International,

37

LLC., Radnor, PA) at room temperature, and then coated with a thin layer of Au for approximately 30s. The SEM investigations on these samples was primarily focused on evaluating the bonding between the filler phase (i.e. clinoptilolite) and the matrix (geopolymer) at high magnifications using 20 KeV accelerating voltage

3.3.6 XRF

Chemical composition of the filler phases, produced water, filtered water and water from the leaching tests (Chapter 5), was characterized with the Rigaku Primus IV Wavelength Dispersive X-ray Fluorescence (WDXRF) spectrometer (Rigaku, Tokyo, Japan) (shown in Figure 3.19). The filler phase samples were studied as fine powders, which were mounted in plastic cup sample holders. The top surface of the powdered samples was covered with 2.5μm thick Mylar thin-film (Chemplex Industries, Inc., Palm City, FL) and is shown in Figure 3.20a. The produced water, filtered water and samples from leaching studies were all liquid samples, and their chemical composition was analyzed to assess the removal of ions dissolved in the produced water during
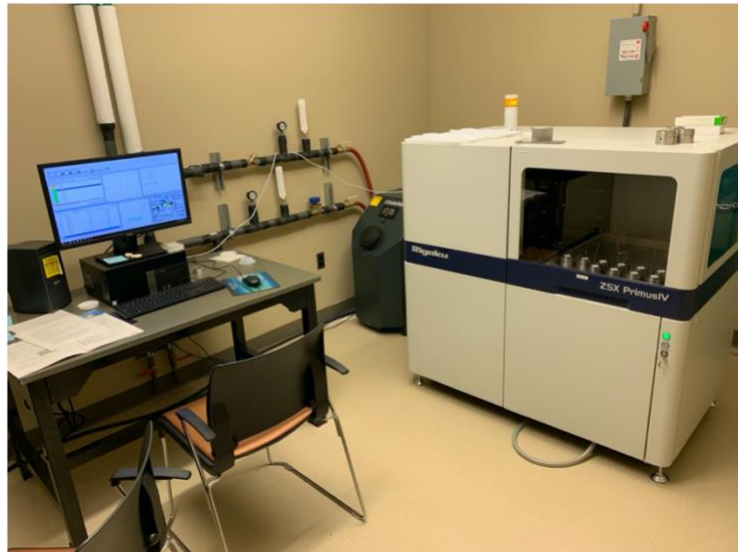
Figure 3.19 Rigaku Primus IV Wavelength Dispersive X-ray Fluorescence (WDXRF) spectrometer (Rigaku, Tokyo, Japan) in the Helmerich Research Center, Core Laboratories was used for determining chemical composition of filler phase, and water samples in this study. .
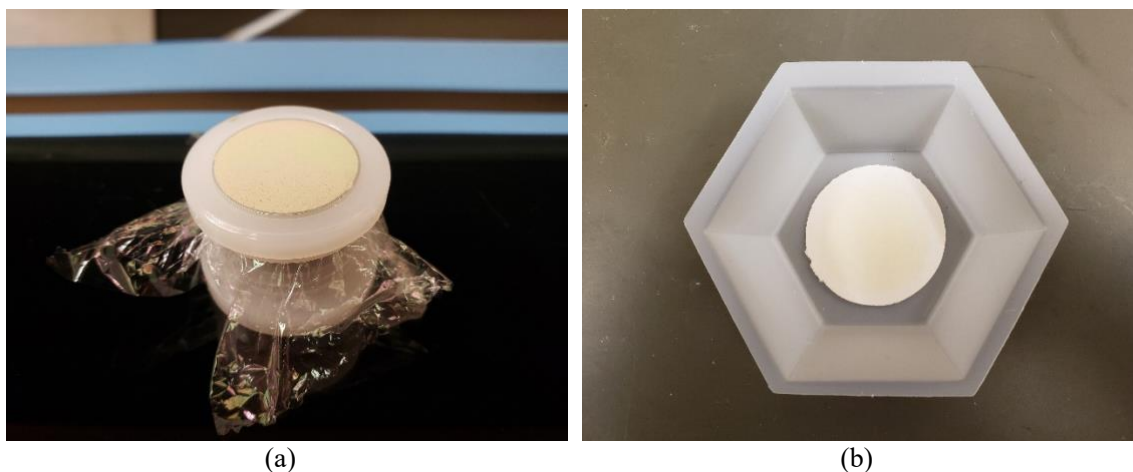
Figure 3.20 Samples for XRF investigations (a) Clinoptilolite powder samples mounted in a plastic holder (20 mm diameter), and covered with a 2.5mm thick Mylar film; (b) 50.8mm diameter Whatman 42 filter paper disk; known volumes of liquid samples was absorbed on these disks and dried.

the filtering step as well as to confirm dissolution of any ions during the leaching tests (for waste encapsulation studies, Chapter 5). Samples for these measurements were prepared by first sampling 200 µl of the solution using a pipette gun, and then spreading the solution evenly over acircular filter paper (Whatman 42, GE Healthcare Life-Sciences, see Figure 3.20b) with a diameter of 50.8 mm. The filter paper was dried at 70°C for 12 hours, and then mounted in the XRF sample holder (30mm diameter window) for analysis. The chemical composition of virgin filter paper was also experimentally determined and used as background levels, which was subtracted from the measurements made on filter paper samples where water/solution had been absorbed. Table 3.6 shows the results of XRF analysis on virgin Whatman 42 filter paper. These values were compared with the nominal chemical composition reported by the filter paper manufacturer, and were found to be different. As filter paper from the same batch was used to determine chemical composition of all solution samples in this study, the experimentally determined values (reported in Table 3.6) were considered adequate and used as background.

Table 3.6 XRF analysis of the virgin Whatman 42 filter paper used in this research.

Elements	Content (ppm)
Cellulose	963000
Zn	31500
I	2750
Fe	1970
Cr	208
Cl	114
Mo	72
Mn	64
Cu	63
Si	62
Ga	52
Al	43
Zr	39
Ca	35
Mg	17
S	10
K	10
Nb	94
Ga	87

3.4 Analytical methods

3.4.1 Porosity and Density

The porosity of the geopolymer and geopolymer composite membrane samples was analyzed by the Archimedes method according to ASTM standard C373-18. This method is commonly used for determination of water absorption and associated properties by (a) vacuum method for pressed ceramic tiles and glass tiles and (b) boil method for extruded ceramic tiles and non-tile fired ceramic whiteware products. As a first step, the test specimens were dried to constant mass by heating in a vacuum oven (VWR Symphony, VWR International, LLC., Radnor, PA) at 70°C and -60 mmHg (-8 kPa) vacuum for 24 hours, followed by cooling in a desiccator. Next, the dry mass,

D, was measured. The specimens were then placed in a small beaker, and positioned inside the Citovac (Struers Inc., Cleveland, OH) chamber. The chamber was them evacuated, and the vacuum (645 mm of Hg, i.e. 0.086 MPa) was maintained for approximately 15 minutes. While maintaining the vacuum, sufficient water was admitted into the beaker to fully submerge the specimens under water. The test specimens were then soaked for approximately 15 minutes, before the vacuum was released and the vessel was returned to atmospheric pressure. Subsequently, the Suspended Mass, S, was determined using the Mettler Toledo weighing balance (Model: XS205DU) and density kit. After the determination of the suspended mass, the specimen was blotted lightly with a damp microfiber cloth to remove all visible water droplets from the surface, and the Saturated mass, M, was measured.

With the dry mass, suspended mass and saturated mass, the parts of the physical properties could be calculated. In the following calculations, the assumption is made that 1 cm_3 of water weighs 1 g.

Exterior volume, V, was calculated in cubic centimeters, as follows:

V = M - S

Volumes of open pores, VOP , and impervious portions, VIP was determined using the following formulae:

VOP = M - D

VIP = D - S

The apparent porosity, P, expressed as a percent, the relationship of the volume of the open pores of the specimen to its exterior volume. The apparent porosity was calculated as follows:

P = [(M - D) / V] × 100

The bulk density, B, in grams per cubic centimeter, of a specimen is the quotient of its dry mass divided by the exterior volume, including pores. The formula used to calculate the bulk density is as follows:

B = D / V

In addition, the density of the coarse, medium and fine zeolites, and the biochar was also determined by the He pycnometry method using the AccuPyc 1340 pycnometer (Micromeritics, Atlanta, GA). At least 30 measurements were made on each powder/granular sample to ensure the reproducibility of the measurements.

3.4.2 Compressive strength

The compressive strength was measured using an Instrton machine according to the ASTM C39/C39M-18. The test was on the Cylindrical samples with ~25.4mm diameter and 21-28 mm height. The top view and side view of samples for compressive test are shown in the Figure 3.21.
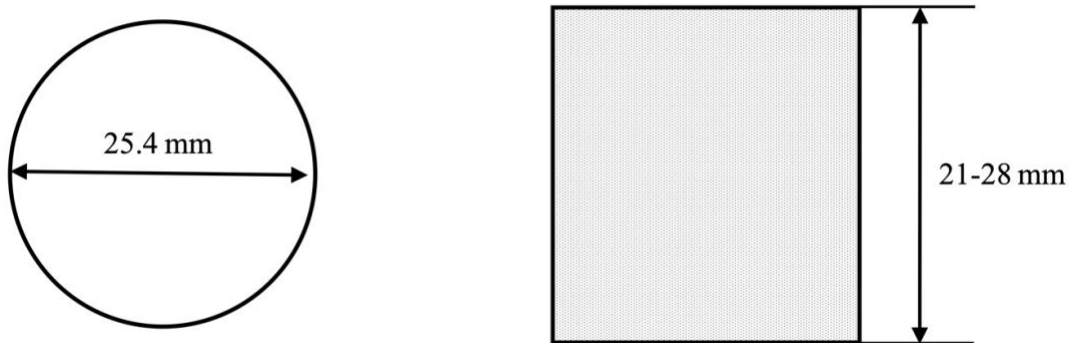
Figure 3.21 Top view and side view of the samples for compressive test.

The diameter used for calculating the cross-sectional area of the test specimen was determined by averaging at least two diameters measured at right angles to each other at about mid height of the specimen. Similarly, the length of the specimen was determined by averaging length values measured at more than three locations spaced evenly around the circumference.
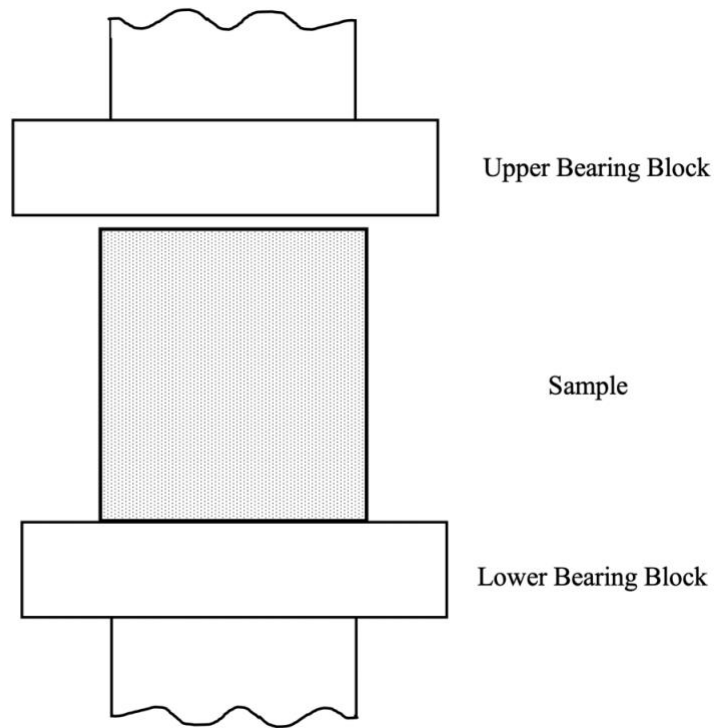
Figure 3.22 Schematic sketch of typical sample loading for compressive strength testing.

For these measurements the cylindrical sample was placed on the lower bearing block of the testing machine such that the axis of the specimen aligned with the center of thrust of the upper bearing block (Figure 3.22). Prior to testing the specimen, it was verified that the load indicator was set to zero. During the testing the load was applied continuously, without shock. The load was applied at a rate of movement (platen to crosshead measurement) corresponding to a stress rate on the specimen of 160 N/s (equivalent to 0.25 MPa/s for the investigated samples). The designated rate of movement was maintained at least during the latter half of the anticipated loading phase. The compressive strength of the specimen was calculated as follows:

$$f_{cm} = \frac{4000 P_{max}}{\pi D^2}$$

f_{cm} = compressive strength, MPa,

P_{max} = maximum load, kN

43

Figure 3.23 (a) Photograph of the Instron Universal Testing System, and (b) Load cell and sample mounting fixtures, used for measuring the compressive strength properties of the geopolymer and geopolymer composites in this study.

Thirty-five samples were tested. The mechanical strength of the samples was tested at the age of 7 day after casting.

CHAPTER IV

GEOPOLYMER MEMBRANES

4.1 Introduction

The purpose of this study was to examine the influence of different types of additive materials on potassium based geopolymers in order to produce inexpensive geopolymer-based filter membranes. The properties and performance of the developed membranes were analyzed for their microstructure, compressive strength, and filtration performance. The microstructure analysis was conducted by microscopic methods (optical and SEM) and by XRF. Potassium based geopolymer with composition of $4SiO_2 \cdot Al_2O_3 \cdot K_2O \cdot nH_2O$ was used as the matrix phase and natural zeolites and biochar were the two types of additives that were explored to process geopolymer composite membranes.

This study was structured in a way to identify optional:

- Geopolymer composition
- Geopolymer curing conditions
- Biochar concentration, and
- Zeolite concentration

for the design of composite ceramic membrane with superior mechanical, microstructure and filtration performance. For this purpose a systematic approach was adopted which in represented in Figure 4.1.

Step #1	Pure Geopolymer $4SiO_2 \cdot Al_2O_3 \cdot K_2O \cdot nH_2O$	**Conditions explored:** ● Composition: n=11 and n=13 ● Curing Temperature T. 40ºC, 60ºC & 80 ºC *Curing Humidity was fixed to 80% relative humidity and curing time was fixed to 5 days.
Step #2	Geopolymer + Biochar	**Conditions explored:** ● Concentration of Biochar. 2, 4, 6 & 10 vol%
Step #3	Geopolymer + Zeolite	**Conditions explored:** ● Zeolite concentration: 20, 40 & 60 vol% ● Zeolite size: Fine, Medium and Coarse

Figure 4.1 Schemcatic illustrating the step-wise approach followed in this study to develop optimal geopolymer based ceramic composite membranes for produced water filtration.

4.2 Processing of geopolymer-based membranes

Pure geopolymer and geopolymer composite slurry mixtures (with additive phases of clinoptilolite or biochar) were prepared following the procedure outlined in Figure 3.9. The slurry was then cast as a 25.4 mm diameter cylinder in a plastic mold, sealed and allowed to cure under predefined conditions. Once cured, the cylindrical sample was removed from the mold and membranes were prepared by sectioning the cured geopolymer composite (or pure) cylindrical sample using a slow action diamond saw (Minitom, Struers, Inc., Cleveland, OH, USA) shown in the Figure 4.2(c) and 4.3.

46

(a)   (b)   (c)
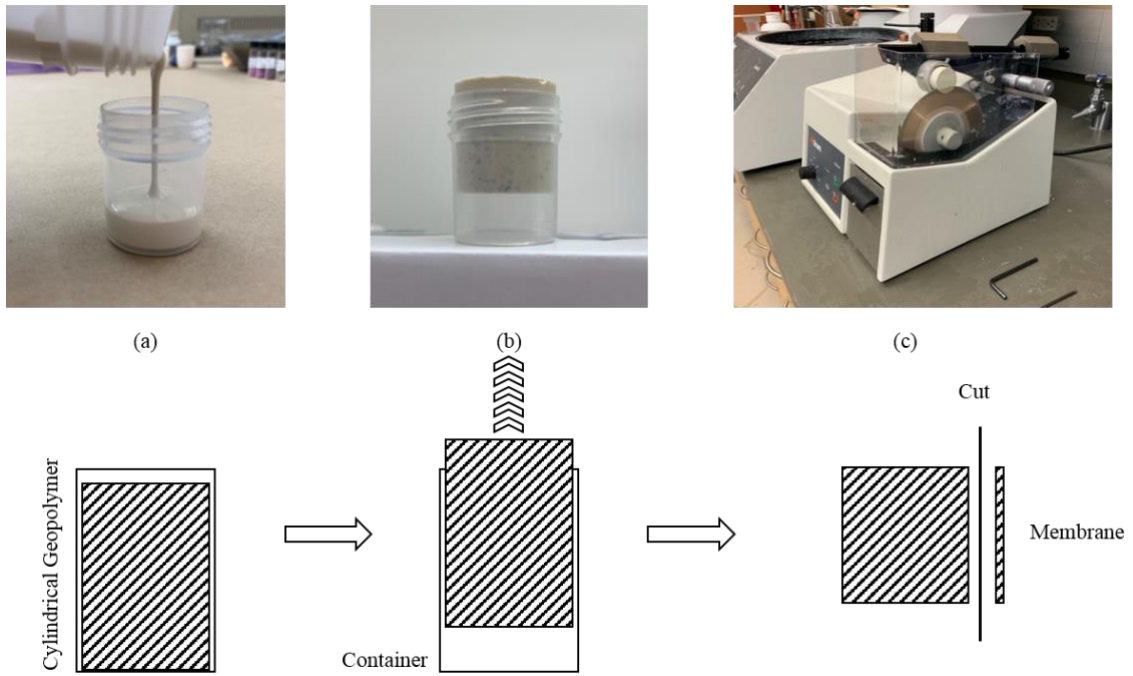
Figure 4.2 Diagram showing the step-wise process for making geopolymer membrane samples.

Figure 4.3 Struers Minitom slow-action diamond saw was used to cut thin membranes from cylindrical cast samples.

4.3 Characterization of geopolymer-based membranes

The processed membranes were characterized for their microstructure, mechanical properties and filtration performance. The details on the methods used for microstructure and mechanical properties characterization were included in Chapter 3. The filtration performance of the membranes was determined using an in-house developed equipment and the details and the procedure used is presented in the following section.

4.3.1 Filtration performance

The filtration performance was evaluated using 25.4 mm diameter membranes of 0.9mm thickness. Figure 4.4 shows an optical image of a virgin geopolymer+zeolite composite membrane. The surface of the membrane was not polished beyond what was obtained by the slow-action diamond cutting action. Table 4.1 lists the physical characteristics of the membranes where porosity was determined by the Archimedes' method. The filtration performance was evaluated by determining the flow rate and filtered water quality (pH, turbidity, TDS concentration, impurity concentration) under a range of applied pressures (see Table 4.2).
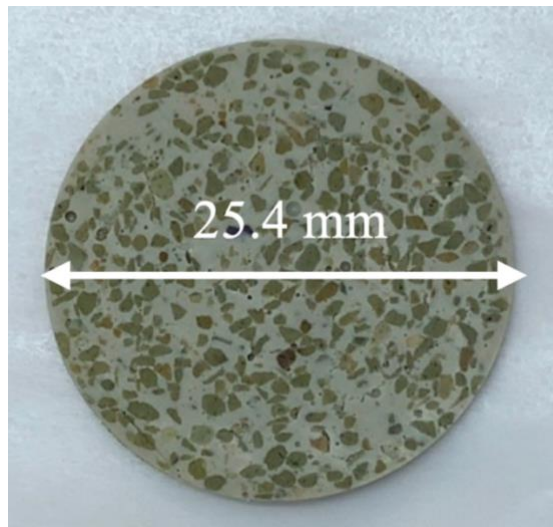
Figure 4.4 Optical image of a geopolymer+zeolite composite member used to test filtration performance.

Table 4.1 Typical physical characteristics of geopolymer membranes used to determine filtration performance.

Characteristics	Values
Appearance	Smooth and clean surface
Dimensions	Diameter: 25.4 mm, Thickness: 0.9mm
Porosity	28% ~ 40%

Table 4.2 Parameters studied in the filtration performance test

Parameters	Value
Pressure	1bar – 9 bar
Time	10 min constant
Flow rate	In ml/min
Turbidity	-
TDS	-
pH	-
Filtered water impurity concentrations (by XRF)	B to U concentrations in ppm

For all of these studies, produced water was used. Turbidity, TDS, pH and impurity concentrations of produced water were analyzed first, and served as a benchmark to evaluate the performance of the membranes as a filter. All the filtration experiments were conducted in dead-end filtration mode, and required application of nominal pressures to "force" produced water through the membranes. For this purpose an in-house filtration set-up was designed, and is shown in Figure 4.5. Filtration set up includes one funnel, two valves and one pipe joint. The membrane was supported on a perforated aluminum metal disc in the specially configured pipe joint, Figure 4.6. Silicone sealant was applied on the edges of the membrane and cured for 30 minutes to prevent any leakage. This ensured that water flowed only through the membrane when pressure was applied. To conduct the filtration test, the vertical column was first filled with produced

water while keeping the Valve 2 closed. Once filled, the Valve #1 was closed and pressure was applied through Valve 2 using pressurized air. Filtered water was collected over a fixed duration of time at the bottom under different pressures and its quantity and quality were determined (see parameters listed in Table 4.2) to evaluate the filtration performance of the tested membrane.
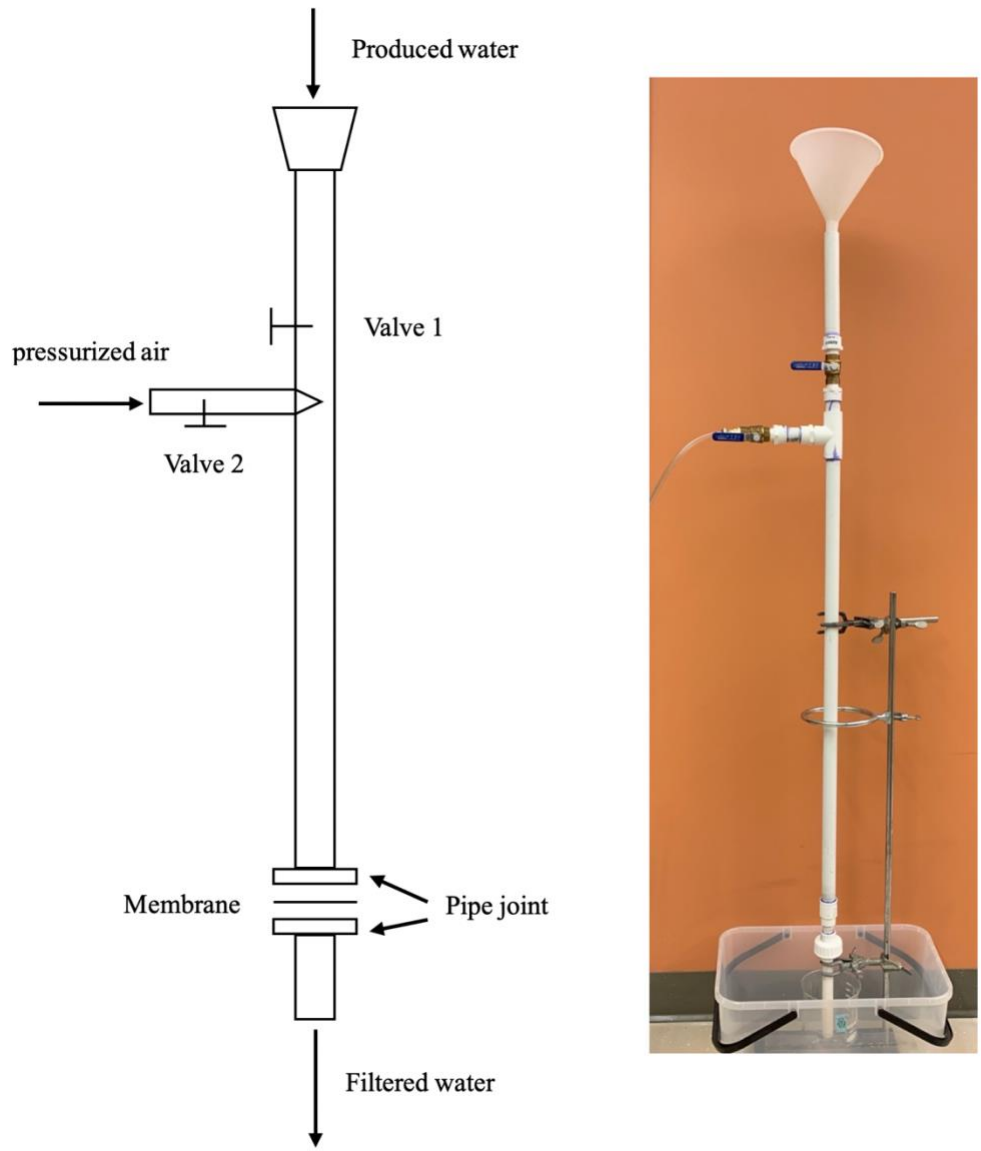
Figure 4.5 Filtration set up design (left) and actual photo (right)
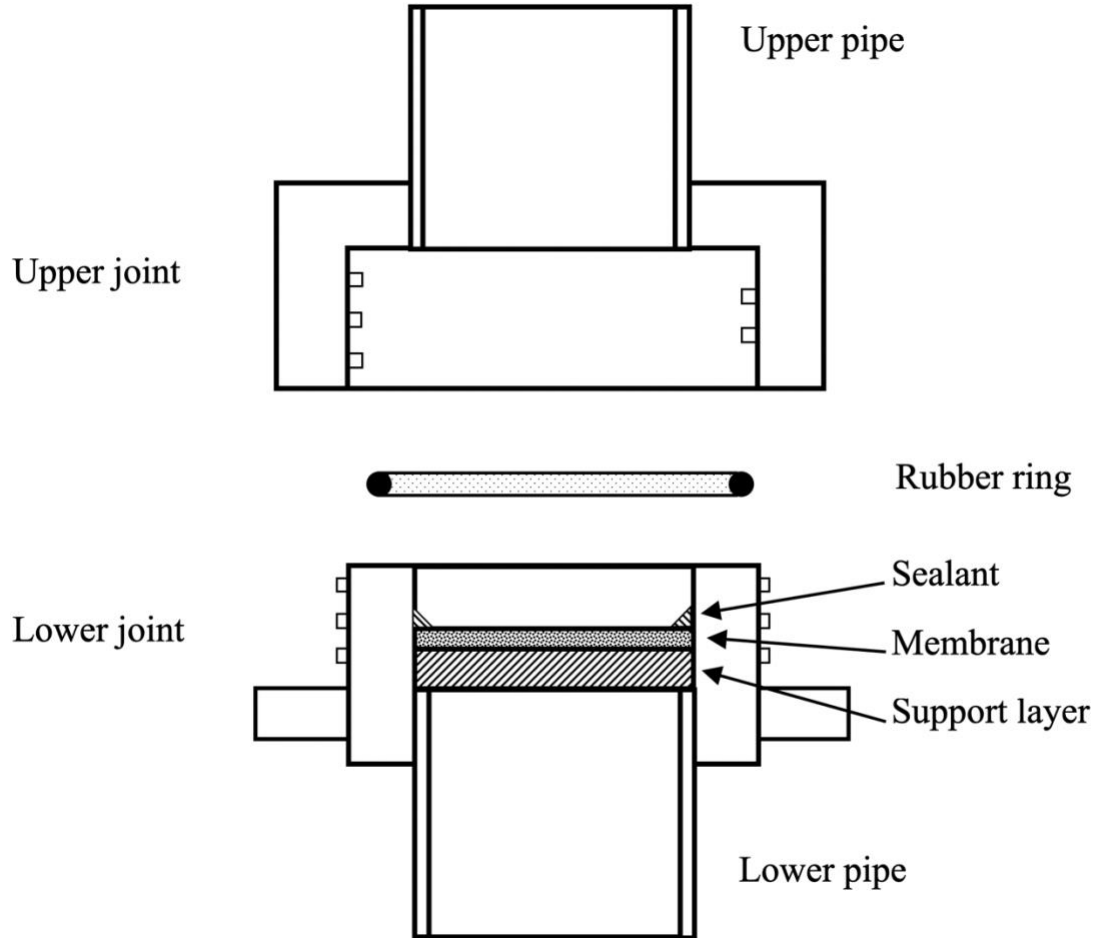
Figure 4.6 Detail diagram of the piper joint and membrane

4.4 Pure Geopolymer membrane

Geopolymer's porosity and pores' size could be controlled by curing temperature and water

content inside the geopolymer. Understanding how to control the pore's size is very important

since the pore's size affects the efficiency of the filtration and determines whether certain ions

could be filtered.

Compositions of geopolymer with different amounts water and different curing

temperatures were synthesized according to the process discussed in sections 3.2 and 4.2. After

synthesis selected membrane samples were characterized for their compressive strength and

filtering performance. In order to determine the optimal composition and processing conditions for the pure geopolymer, the samples and conditions shown in the Table 4.3 were studied.

Table 4.3 Composition and processing conditions evaluated for the pure geopolymer membrane samples

Water Content "n" (moles)	Curing Temperature (°C)	Chamber Humidity (%)	Curing Time Days)
11	60	80%	5
13	40	80%	5
13	60	80%	5
13	80	80%	5

After five days of curing, the geopolymer samples cured at 40°C were still not solidified. It was observed that samples cured at low temperatures i.e. 40°C needed more time to react than those samples which curried at higher temperatures i.e. 60°C and 80°C). On the other hand, samples curried at 80 °C, on the other hand showed cracks on the surface. This was most likely due to rapid loss of water from the surface at higher temperatures. Therefore, 60°C was identified as the optimal temperature for curing the geopolymer membrane samples.
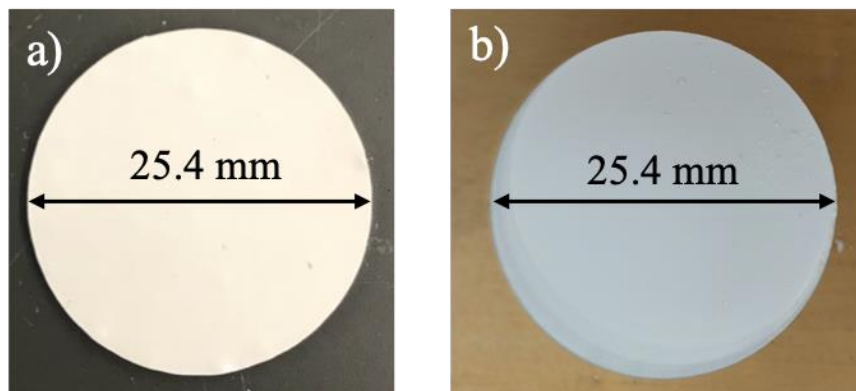
Figure 4.7 Pure geopolymer membrane samples cured at 60°C for a) 11 mol water and b) 13 mol water compositions.

4.4.1 Compressive strength and flow properties of pure geopolymer membrane samples

Pure geopolymer samples with 11 and 13 mol water content, and cured at 60°C for five days were tested for their compressive strength properties as well as for flow performance. Compressive strength was determined on cylindrical samples, approximately 28 mm in diameter and 22 mm in height. The details on the testing procedures were included in section 3.4.2. Measurements were made on at least three samples and average values are reported in Table 4.4. Flow properties were measured on membrane samples, approximately 25 mm in diameter and 0.9 mm in thickness, following the procedures presented in section 4.3.1.

Table 4.4 Compressive strength and water flow rate of pure geopolymer membrane samples cured at 60°C for 5 days

Water Content "n" (moles)	Sample Diameter (mm)	Sample Height (mm)	Compressive Strength (MPa)	Water Flow Rate at 0.3MPa (ml/min)
11	28.56	21.42	21.40±3.39	0.013
13	29.42	23.81	23.96±2.19	0.707

Based on the compressive strength and water flow rate measurements, pure geopolymer samples processed with 13 moles of water had superior compressive strength as well as flow properties. However, these samples were found to be unstable when left outside in the open, and developed cracks. Comparable properties of the sample processed with 11 moles of water were considered adequate for the purpose of this study. Hence, 11 moles of water was selected as optimum composition for the geopolymer matrix phase to process geopolymer composite membranes for further studies. Based on these investigations on the pure geopolymer samples, curing conditions were decided as 60°C for 5 days for all geopolymer composite samples.

4.5 Effect of biochar addition on properties of geopolymer composite membranes

Biochar was explored as an additive to the geopolymer to process composite membranes. Due to superior adsorption properties biochar is widely used in water purification applications. In this study, addition of biochar was expected to enhance the filtration capabilities of the pure geopolymer phase. However, the effect of biochar addition on the compressive strength and flow rate properties of the composite membranes were unknown. Therefore, a comprehensive experimental study was devised to examine the effect of biochar addition on the compressive strength and the filtration performance. Table 4.5 provides the details on the range of biochar content that was added and the processing conditions that were used to process and test the geopolymer+biochar composite membranes.

Table 4.5 Geopolymer with biochar membrane samples investigated in this study.

Biochar Content (vol %)	Water Content "n" (moles)	Curing Temperature (ºC)	Humidity (%)	Curing Time (Days)
2%	11	60	80%	5
4%	11	60	80%	5
6%	11	60	80%	5
10%	11	60	80%	5

Calculated amount of biochar powder was weighed and mixed with the pure geopolymer slurry according to the preparation process discussed in section 3.2 for each of the compositions included in Table 4.5 (i.e. for 2, 4, 6 and 10 vol%). After the curing, the cylindrical samples were either tested for their compressive strength properties, or were cut into thin discs (0.9mm thickness). Samples of geopolymer+biochar composite membranes are shown in the Figure 4.9.
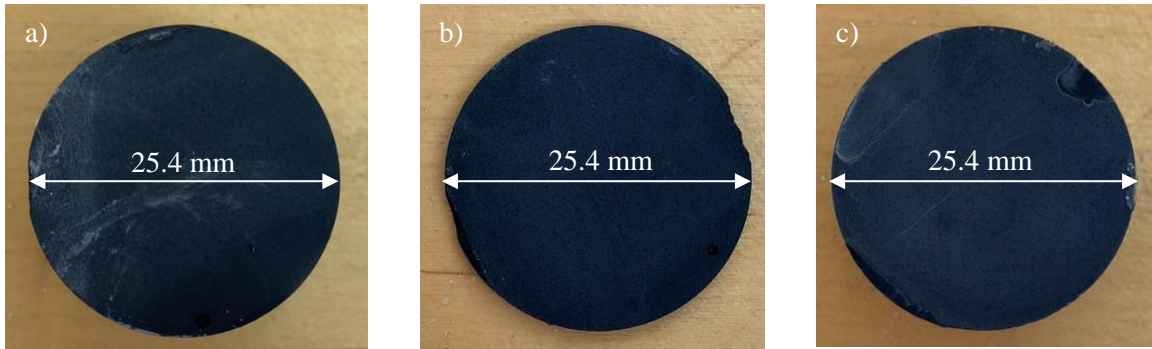
Figure 4.8 Geopolymer + biochar membrane samples cured at 60°C for a) 2 vol%, b) 4 vol% and c) 6 vol% compositions.

As biochar absorbed significant amounts of water from the geopolymer slurry, the resulting slurry was very viscous which made casting very difficult. More importantly, reduced amount of water was available for the geopolymerization reaction, and resulted in fragile samples. Examination of the surface of a small piece from the geopolymer+biochar sample prepared with 10 vol% biochar was conducted using the optical microscope. As shown in Figure 4.10, the sample had excessive
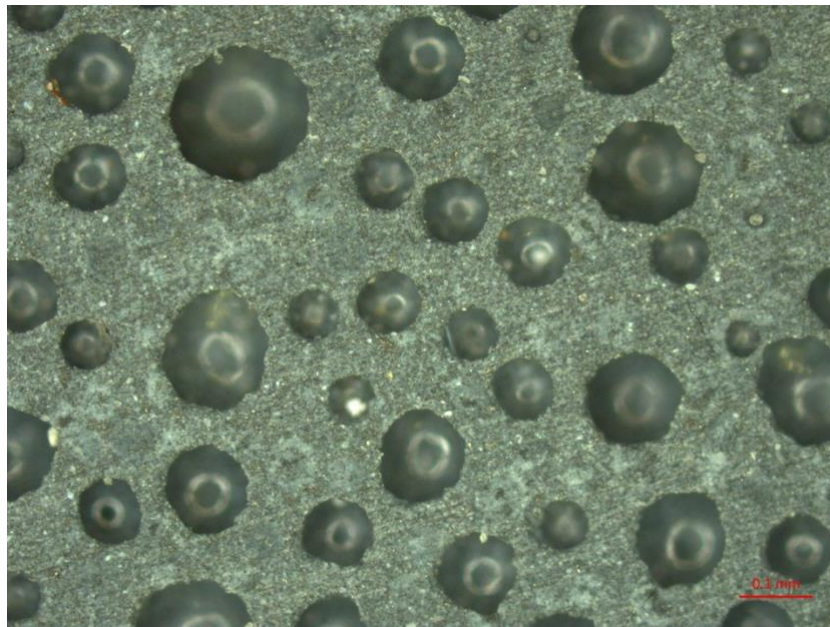
Figure 4.9 Optical micrograph of the geopolymer+biochar composite membrane with 10 vol % biochar.

number of large pores (approximately 1 mm diameter). Therefore, it was decided to restrict the biochar addition to less than 10 vol% and only geopolymer+biochar samples with 2 vol%, 4 vol%, and 6 vol% were further investigated for their mechanical and filtration performance.

4.5.1 Effect on the compressive strength

Addition of biochar significantly deteriorated the compressive strength of the geopolymer+biochar composites. Table 4.6 shows the effect of biochar addition on the compressive strength of geopolymer membrane. As can be seen, addition of 2 vol% of biochar did not have much effect on the compressive strength when compared with the pure geopolymer sample. However, addition of 4 vol% and 6 vol% reduced the compressive strength by about 33% and 37%, respectively.

Table 4.6 Compressive strength of geopolymer + biochar composite samples

Sample	Sample Diameter (mm)	Sample Height (mm)	Compressive Strength (MPa)
Pure Geopolymer	28.56	21.42	21.40±3.39
2 vol% Biochar	29.36	23.81	21.72±1.69
4 vol% Biochar	29.62	27.49	14.16±0.86
6 vol% Biochar	29.45	28.41	13.42±0.34

4.5.2 Effect on filter performance

The filtration performance of the geopolymer+biochar membranes was evaluated for composite samples with 2 vol%, 4 vol%, and 6 vol % biochar. The membrane discs (25.4 mm diameter, and 0.9 mm thick) were supported on aluminum perforated discs for these tests (see section 4.3.1). The membrane with 4 vol% biochar cracked during the test, and was not pursued further. Results on the produced water and the filtered water composition, as determined using the XRF, are shown in Table 4.6 for the membranes with 2 vol%, and 6 vol % biochar. Based on these studies,

Table 4.6 XRF results of produced water before and after filtration using the geopolymer+biochar composite membranes (unit: ppm).

Sample	Ca	Zn	Mg	Sr	Br	Fe	K	Si	S
Before Filtration	15900	3290	2410	1030	780	309	289	47.5	33.9
2 vol% Biochar	16100	2360	2190	944	750	107	4140	69.9	31.1
Before Filtration	20200	17600	2480	1040	811	2720	242	39.0	51.1
6 vol% Biochar	20500	16300	2500	1000	772	5330	2240	31.0	37.4

it was observed that the geopolymer+biochar composite membranes could reduce, although marginally only, the concentration of larger cations including Sr, Br, and Fe. There was unremarkable change in the concentration of the cations such as Ca, Zn, Mg, and S. The observed increase in the concentration of K and Si cations in the filtered water is most likely due to their leaching from the geopolymeric matrix phase. Therefore it was concluded that geopolymer+biochar composite membranes are not adequate for filtration of produced water.

4.6 Effect of zeolite addition on properties of geopolymer membranes

The structure of geopolymer is very close to the structure of zeolites but without regular ordering to longer distance – it has amorphous character. The clinoptilolite zeolite, $Na_6[Al_6Si_{30}O_{72}]24H_2O$, like kaolinite ($Al_2SiO_5(OH)_4$) is hydrated aluminosilicate phase. Metakaolin, on the other hand, is dehydroxyalted kaolinite, lacks any long range ordering and shows enhanced reactivity towards alkali silicate solutions to form the geopolymer phase. Due to the similarity in chemical composition of clinoptilolite and metakaolin, clinoptilolite is expected to demonstrate some reactivity with the alkali silicate solutions, at least at the interface. Therefore, it was a suitable additive for geopolymber based composite ceramic membranes. An additive with microporous channels, which can bond well with the geopolymer matrix phase, can enhance the strength and

the enable improved filtration properties of the geopolymeric phase. This hypothesis formed the basis for exploring the clinoptilolite as an additive phase in geopolymers to develop ceramic composite filtration membranes. Table 4.7 provides the details on the range of commercial clinoptilolite type and content that was added to the pure geopolymer phase, and the processing conditions that were used to process and test the geopolymer+zeolite composite membranes.

Table 4.7 Geopolymer with zeolite membrane samples

Zeolite		Water Content "n" (moles)	Curing Temperature (ºC)	Chamber Humidity	Curing Time (Days)
Granularity	Percentage				
Fine	20%	11	60	80%	5
Fine	40%	11	60	80%	5
Medium	20%	11	60	80%	5
Medium	40%	11	60	80%	5
Coarse	20%	11	60	80%	5
Coarse	40%	11	60	80%	5

Calculated amount of zeolite particles was weighed and mixed with the pure geopolymer slurry according to the preparation process discussed in section 3.2 for each of the compositions included in Table 4.7. After the curing, the cylindrical samples were either tested for their compressive strength properties, or were cut into thin discs (0.9 mm thickness). Samples of geopolymer+zeolite composite membranes are shown in the Figure 4.10. During the cutting of geopolymer+coarse zeolite sample, the coarse zeolite particles would often pull-off from the membrane, an example is shown in the Figure 4.10 (e). This observation was unique to the coarse zeolite composite membranes only, and was not observed in the case of fine or medium zeolite composites. It is possible that the low surface area of the coarse zeolite particles available for reaction with the geopolymer phase results in weaker bonding, and allows easier pull-out of the coarse zeolite particles from the geopolymer matrix.

58
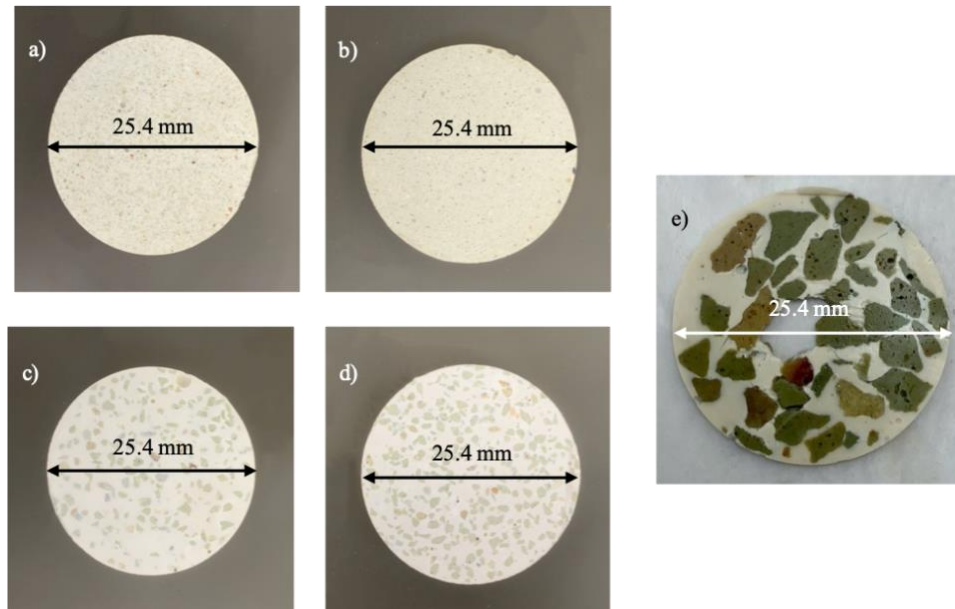
Figure 4.10 Geopolymer + zeolite membrane samples for a) Fine 20 vol%, b) Fine 40 vol%, c) Medium 20 vol%, d) Medium 40 vol% and e) Coarse 40 vol% zeolite compositions.

Examination of the surface of a small piece from the geopolymer+zeolite sample prepared with 10 vol% fine zeolite did not reveal any particle pull-out. However, as shown in the optical micrograph in Figure 4.11, the sample had excessive number of large pores (approximately 0.03-0.1 mm diameter). In order to verify the bonding of the zeolite particles and the geopolymer matrix a small piece from the geopolymer+zeolite sample prepared with 20 vol% medium zeolite

Figure 4.11 Optical micrograph of the geopolymer+zeolite composite membrane with 10 vol % fine zeolite.
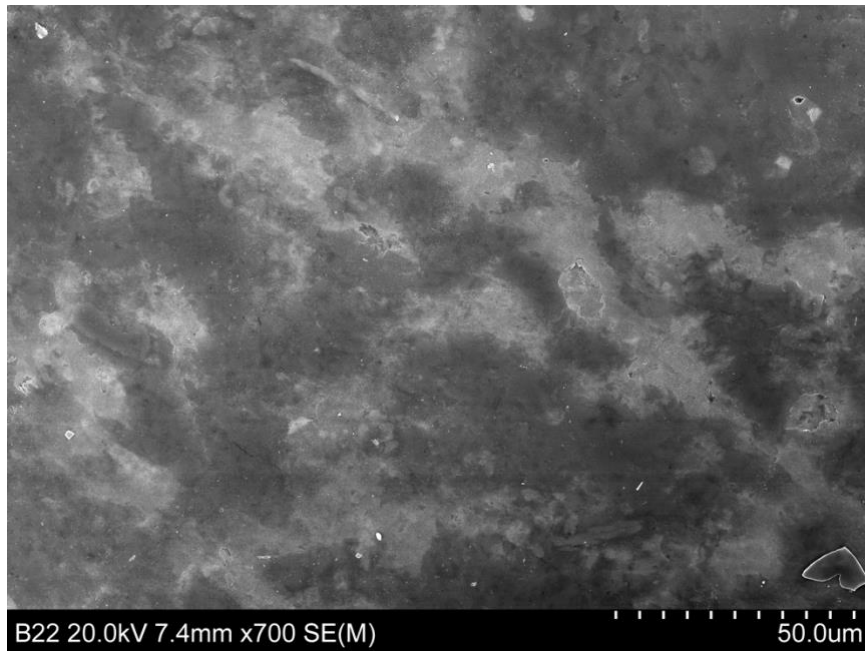
(a)
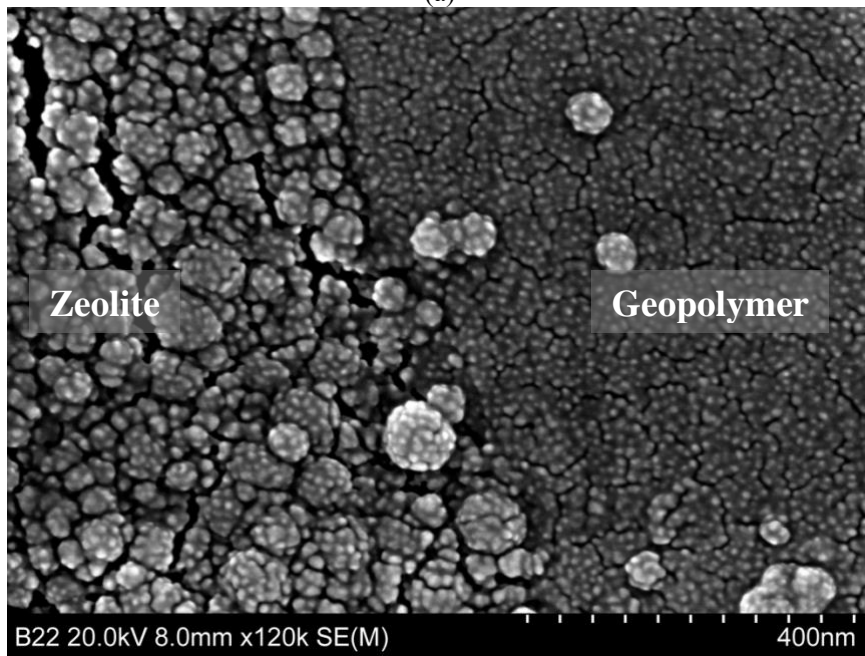
(b)

Figure 4.12 SEM images of the virgin geopolymer+zeolite composite membrane with 20 vol % fine zeolite at magnification (a) 700 X, and (b) 120000 X.

was examined using the SEM. As shown in Figure 4.12, zeolite and geopolymer were seamlessly connected with each other. The gap between the zeolite and geopolymer is $\leq$ 15-20 nm.

4.6.1 Effect on the compressive strength

Addition of zeolite significantly improved the compressive strength of the geopolymer+zeolite composites. Table 4.8 shows the effect of zeolite addition on the compressive strength of geopolymer composite. At least five samples were tested for each composition and the values reported are average values. Figure 4.13 is a graphical comparison of the compressive strength of the pure geopolymer sample and the various geopolymer+zeolite composite samples. As can be seen, addition of 20 vol% of fine zeolite had a remarkable effect on the compressive strength when compared with the pure geopolymer sample. No change was observed in the compressive strength of the composite with 20 vol% of medium zeolite from that of the pure geopolymer sample. Increase in the volume percentage of the fine and medium zeolite to 40%, however, decreased the compressive strength of the geopolymer+zeolite composites. Addition of coarse zeolite particles, in contrast, significantly deteriorated the compressive strength properties. Based on these observations, the composite samples with coarse zeolite particles were not considered suitable for membrane applications, and were not considered for filtration performance studies. Geopolymer with 20 vol% of fine zeolite sample had the highest compressive strength.

Table 4.8 Results from compressive strength tests on geopolymer+zeolite samples

Zeolite		Sample	Sample	Compressive
Granularity	Percentage	Diameter (mm)	Height (mm)	Strength (MPa)
Fine	20%	29.33	24.22	32.20±7.19
Fine	40%	29.40	26.88	21.82±4.41
Medium	20%	29.38	23.60	21.43±1.86
Medium	40%	29.50	26.42	14.19±3.45
Coarse	20%	29.39	23.00	11.87±4.77
Coarse	40%	29.88	27.44	11.48±4.97
Pure Geopolymer	0%	28.56	21.42	21.40±3.39
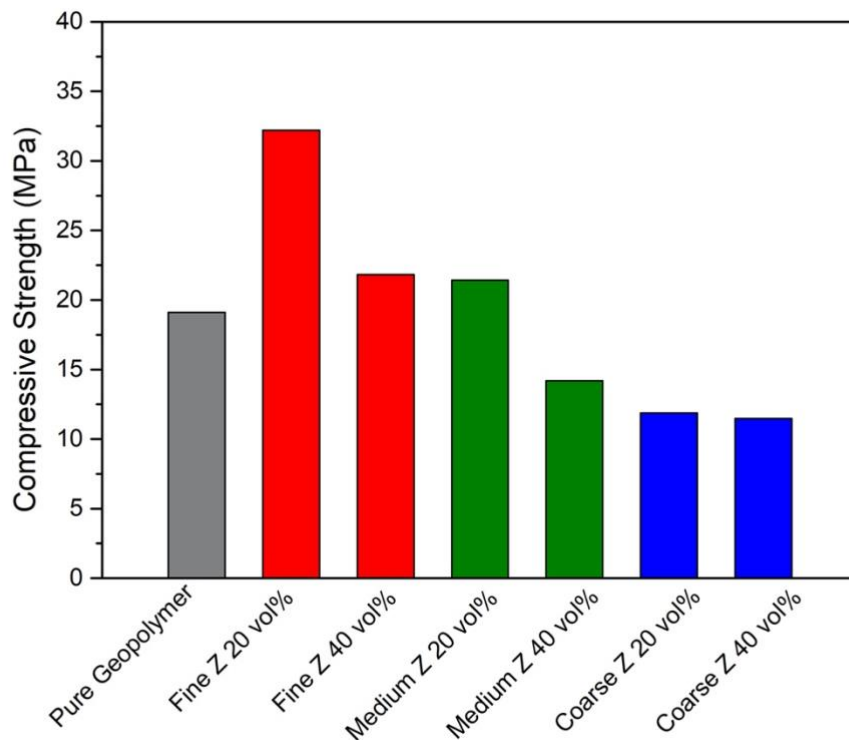
Figure 4.13 Graphical comparison of the compressive strength of pure geopolymers with geopolymer+zeolite samples with different types and concentration of zeolite particles.

4.6.2 Effect on filter performance

The produced water flow rate observed for the fine and medium zeolite particle geopolymer composite membranes is compared with the pure geopolymer membranes in Figure 4.14. The geopolymer composite membrane with 40 vol% of fine zeolite had the highest flow rate. Although composite samples with 20 vol% of fine/medium zeolite particles or with 40 vol% of medium zeolite have lower compressive strength than pure geopolymer sample, they had significantly higher flow rate than pure geopolymer membrane sample. The composite sample with 20 vol % of fine zeolite, on the other hand, had cracked at 0.4 MPa of applied pressure. This could be due to the variance in the presence of flaws from one sample to another of the same composition. With the

higher compressive strength, it is expected that the membrane samples can withstand higher

pressures, thereby permitting a higher flor rate.
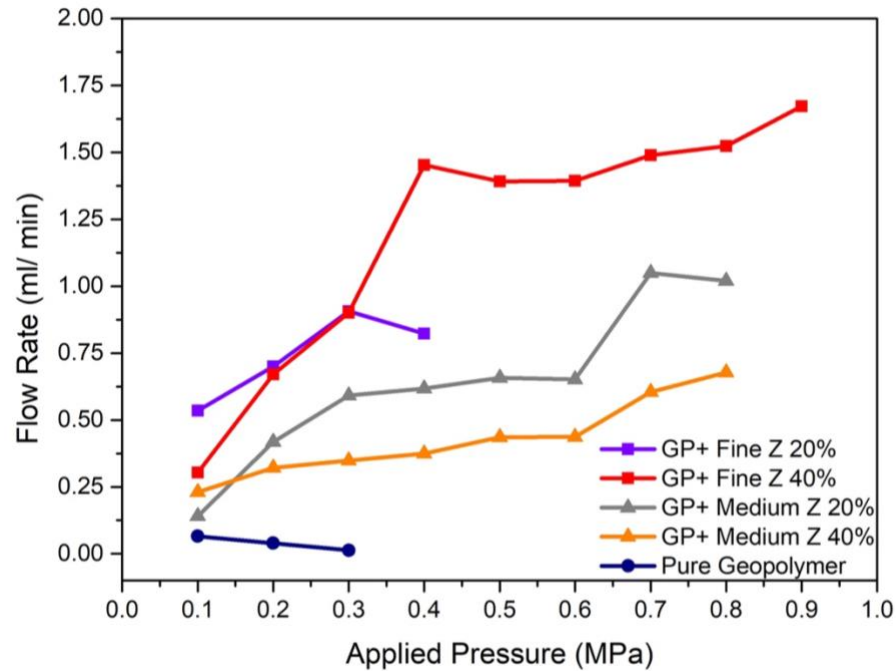
Figure 4.14 Water flow rate of geopolymer with zeolite samples

Besides the flow rate measurements, the ability of the membrane to remove impurities, both

particulate as well as dissolved, was evaluated by examining the membrane with optical

microscope, by SEM/EDS and by measuring the change in water quality. Figure 4.15 shows the
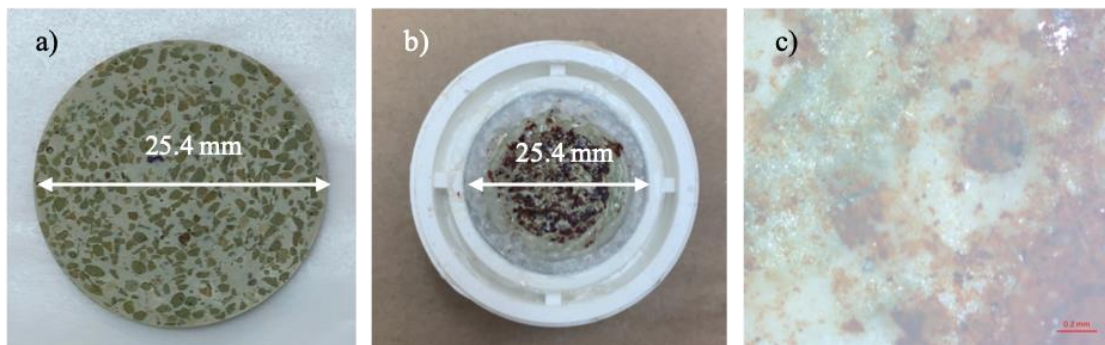
Figure 4.15 Before and after filtration image of the same geopolymer composite membrane with
medium 40 vol% zeolite. a) Membrane before filtration b) c) Membrane after filtration.

optical images of surface of the same filter membrane before and after filtration. The retention of the brown colored particles on the membrane surface is clearly seen in Figure 4.15 (b) and (c). The produced water before and after filtration through a geopolymer composite membrane with 20 vol% medium zeolite is shown in the Figure 4.16. The change in turbidity, pH and TDS upon filtration through the geopolymer+zeolite composite membranes under different pressures is presented in Table 4.9. Before filtration, the turbidity of the produced water was 74.7 NTU. After filtration through pure geopolymer membrane at 0.1 MPa (1 bar) pressure, the turbidity of the produced water was reduced by approximately 90% to 7.92 NTU. This confirmed that almost all visible particles floating in the produced water were filtered. Turbidity values after filtration through the geopolymer+zeolite composite membranes, however, ranged between 4.32 and 15.95 NTU for all the membranes tested (see Table 4.9). The pH of produced water was tested at 4.12, and after filtration through any of the membranes it increased to values ranging between 5.35 and 6.65. No specific trend in change in pH was observed with pressure or membrane type. The increase in the pH after filtration is most likely due to unreacted KOH present in the geopolymer
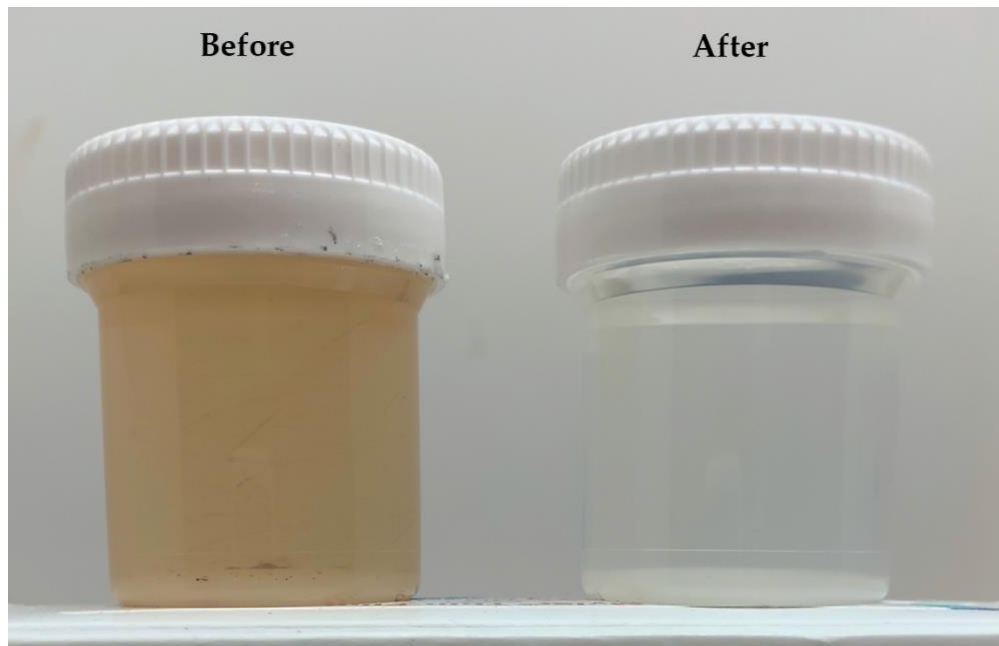
Figure 4.16 Produced water before and after filtration of geopolymer with medium 20 vol% membrane at 0.1MPa pressure.

phase of the membranes. The TDS of produced water was measured at 65100 ppm, and unremarkable change was observed upon filtration through the membranes. This confirmed that the membranes were unable to separate out the chloride or the sodium ions, which constitute the major components that contribute towards the high TDS concentrations observed for produced water.

The XRF results of produced water before and after filtration through the geopolymer+zeolite membranes using 0.1 MPa pressure are shown in the Table 4.10. The percentage of ions removed is included in Table 4.11 for each membrane type. These results further confirm the observed changes in the pH and TDS. Significant reduction in the concentrations of all ions except K was observed after filtration through the fine zeolite composite membranes. The filtration performance of the fine zeolite composite membranes, in terms of removal of each element, improved by increasing the concentration of the fine zeolite particles form 20 vol% to 40 vol%. The only exception to this was the Si content, which may be biased by unusually high Si concentration in the produced water. It is possible that presence of some sand particles in the produced water sampled for the XRD analysis could have resulted in the unusually high Si content for that sample. The filtration performance of the membrane samples with medium zeolite was much inferior to the fine zeolite composite membranes. However, removal of Fe and P from produced water using these membranes was comparable to the fine zeolite composite membranes. In increase in the K concentration of water after filtration is attributable to dissolution of unreacted KOH from the geopolymeric phase of the composite membranes, and is consistent with the increase in pH observed, as discussed earlier. Overall, these results indicate that the filtration performance of geopolymer composite membranes with fine zeolite is better than geopolymers with medium zeolite.

Table 4.9 Changes in turbidity, TDS and pH observed after filtration through the geopolymer+zeolite composite membranes under pressure.

Sample	Parameter	Pressure (bar)							
		1	2	3	4	5	6	7	8
Pure Geopolymer	Turbidity (NTU)	7.92							
	TDS (1000 ppm)	54.2							
	pH	5.607							
Fine 20 vol%	Turbidity (NTU)	7.82	4.38	6.54	5.13				
	TDS (1000 ppm)	>60	54.2	>60	>60				
	pH	5.607	6.342	5.793	5.347				
Fine 40 vol%	Turbidity (NTU)	12.17	13.13	10.59	15.95	16.51	12.87	14.31	13.43
	TDS (1000 ppm)	55.1	57.8	>60	57.4	59.3	>60	>60	>60
	pH	5.492	5.426	6.492	6.643	5.945	6.221	6.137	6.654
Medium 20 vol%	Turbidity (NTU)	9.37	5.43	6.24	7.14				
	TDS (1000 ppm)	>60	54.7	>60	>60				
	pH	5.677	5.939	5.427	5.631				
Medium 40 vol%	Turbidity (NTU)	7.27	4.32	6.59	8.37				
	TDS (1000 ppm)	58.7	>60	51.3	>60				
	pH	5.879	5.931	6.434	6.471				

Table 4.10 XRF results of water tested before and after filtration through the geopolymer+zeolite composite membranes at 0.1 MPs pressure (unit: ppm).

Sample	Water pressure	Cl	Na	Ca	Zn	Fe	Mg	Sr	P	S	Br	K	Si
Fine 20 vol%	Before	91800	38300	15700	3570	254.0	2250	953	60.70	29.2	717	213	1250
	0.1 MPa	80400	28200	7230	1670	56.6	1100	302	4.90	18.6	477	1080	77.4
Fine 40 vol%	Before	168000	106000	20600	3810	183.0	2980	1160	56.20	40.9	805	479	74.2
	0.1 MPa	108000	70400	11000	89.7	55.8	1430	592	3.80	18.4	525	6310	48.3
Medium 20 vol%	Before	98600	81800	17100	4250	238.0	2490	1060	49.90	36.4	806	440	50.3
	0.1 MPa	91700	38200	15000	2660	60.0	2410	1010	4.36	27.4	791	4020	45.2
Medium 40 vol%	Before	15000	91900	18400	7730	374.0	2660	1000	52.10	53.8	724	241	58.7
	0.1 MPa	14200	87700	17400	1890	83.4	2300	952	5.18	32.3	701	1480	26.4

Table 4.11 The removal rate of different elements from produced water by the four geopolymer+zeolite composite membranes. These results are based on values reported in Table 4.10.

Sample	Cl	Na	Ca	Zn	Fe	Mg	Sr	P	S	Br	K	Si
Fine 20 vol%	12.4%	26.4%	53.9%	53.2%	77.7%	51.1%	68.3%	91.9%	36.3%	33.5%	-507.0%	99.4%
Fine 40 vol%	35.7%	33.6%	46.6%	97.6%	69.5%	52.0%	49.0%	93.2%	55.0%	34.8%	-1317.3%	34.9%
Medium 20 vol%	7%	53.3%	12.3%	37.4	74.8%	3.2%	4.7%	91.3%	24.7%	1.9%	-93.6%	10.1%
Medium 40 vol%	5.3%	4.6%	5.4%	75.5%	77.7%	13.5%	4.8%	90.1%	40.0%	3.2%	-641.1%	55.0%

Besides evaluating the concentration of different ions in the filtered water it was of interest to observe surface of the membranes to identify particles that were retained. For this purpose, sections of the membranes which had been subjected to filtration studies at various pressures, were analyzed using the SEM. In addition, elemental distribution on the surface of the membranes was also mapped using the EDS. The results of these investigations are summarized in Figures 4.17 through 4.20, with each figure corresponding to a specific geopolymer+zeolite composite membrane. Each one of the tiled images in the bottom half of each figure shows distribution of a specific element in the examined region of the filter, while the top larger size image shows the SEM image of the analyzed region. It should be reiterated that the virgin membranes comprise of a distribution of the clinoptilolite zeolite particles with composition $Na_6[Al_6Si_{30}O_{72}]24H_2O$ (along with Ca, Al, K, Fe and some impurities, see Table 3.4), in the geopolymeric matrix phase which is best represented as $4SiO_2.Al_2O_3.K_2O.11\ H_2O$. Therefore, elements such as Al, Si, and K are expected to overlap and be widely distributed as seen in all the figures, and is most clearly seen at low magnification in Figure 4.19. The presence of different particles and their approximate composition is also evident from this analysis. For example the correspondence of Na and Cl in Figure 4.17 strongly indicates that the particle being observed was a NaCl salt particle. Similarly, Figure 4.18 suggests that the particle was rich in Fe, Ca, Si and O. The presence of a $BaSO_4$ particle in Figure 4.20 is supported by the common region shared by Ba, S and O. Interestingly Ba was not detected at other locations, and perhaps is present only as particles of its sulfate compound.
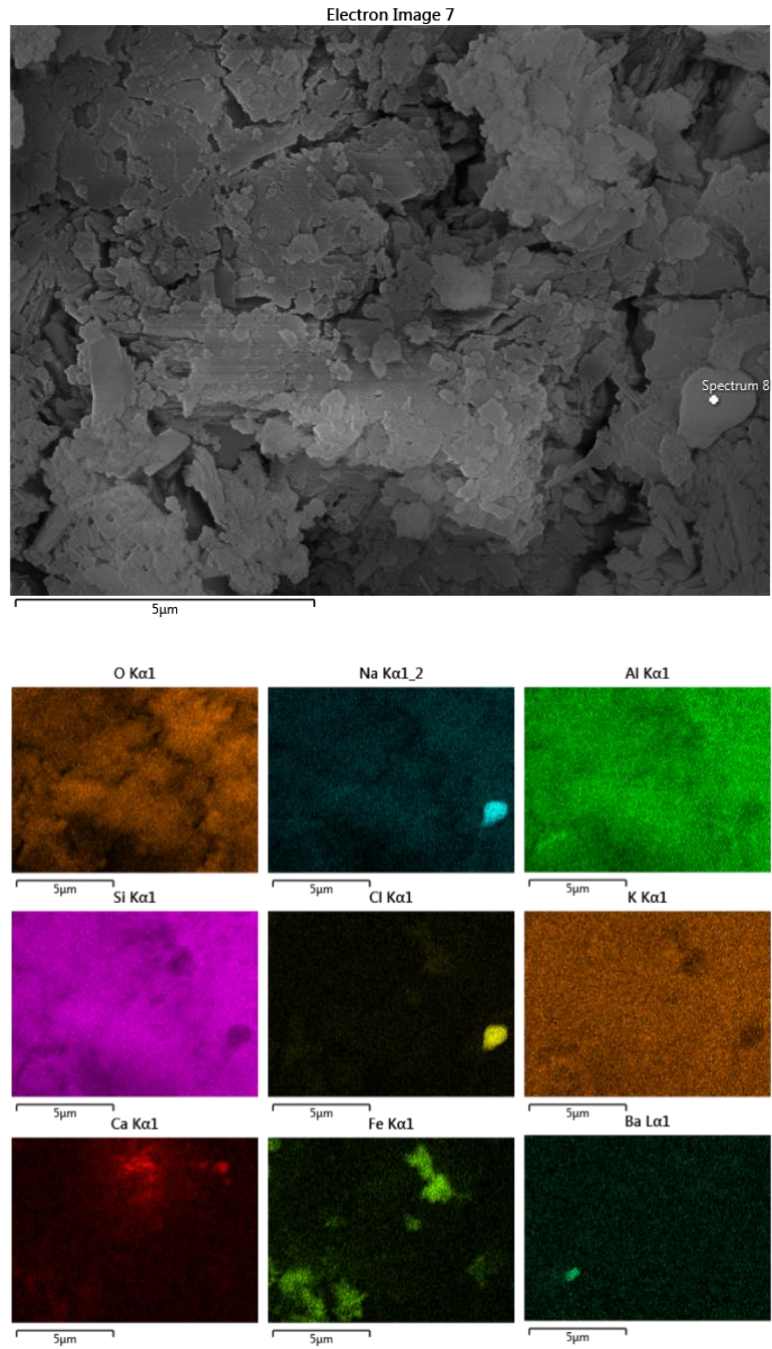
Figure 4.17 EDS mapping of geopolymer + fine 20% zeolite sample at 10,000x magnification.
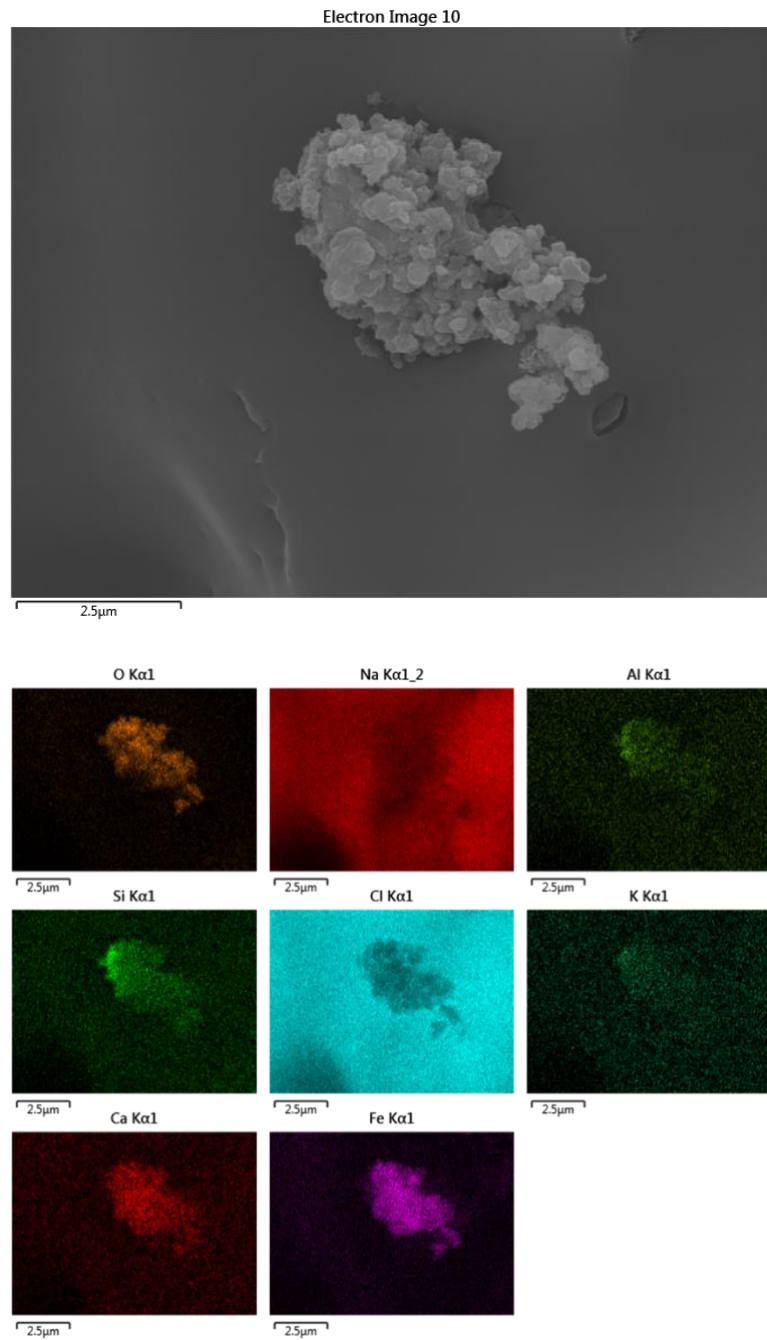
Figure 4.18 EDS mapping of geopolymer + fine 40% zeolite sample at 11,000x magnification.
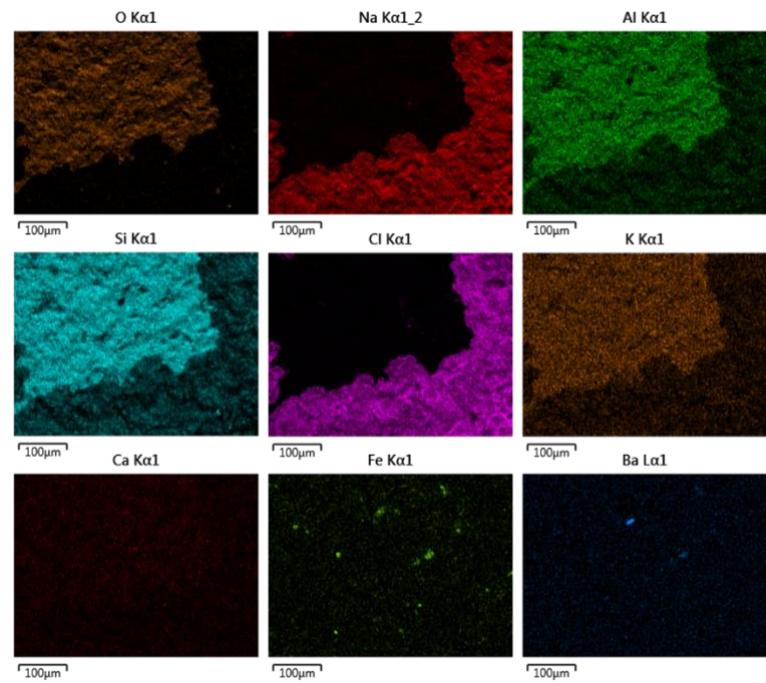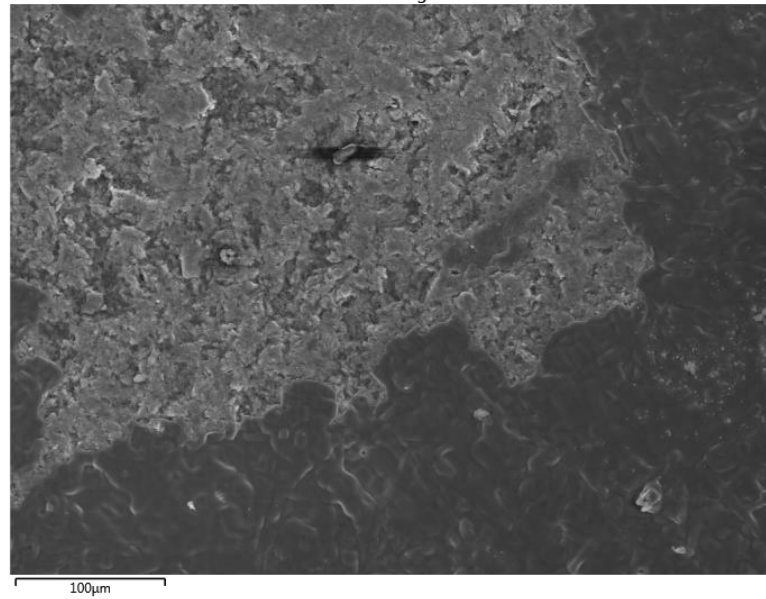
Figure 4.19 EDS mapping of geopolymer + medium 20% zeolite sample at 250x magnification.
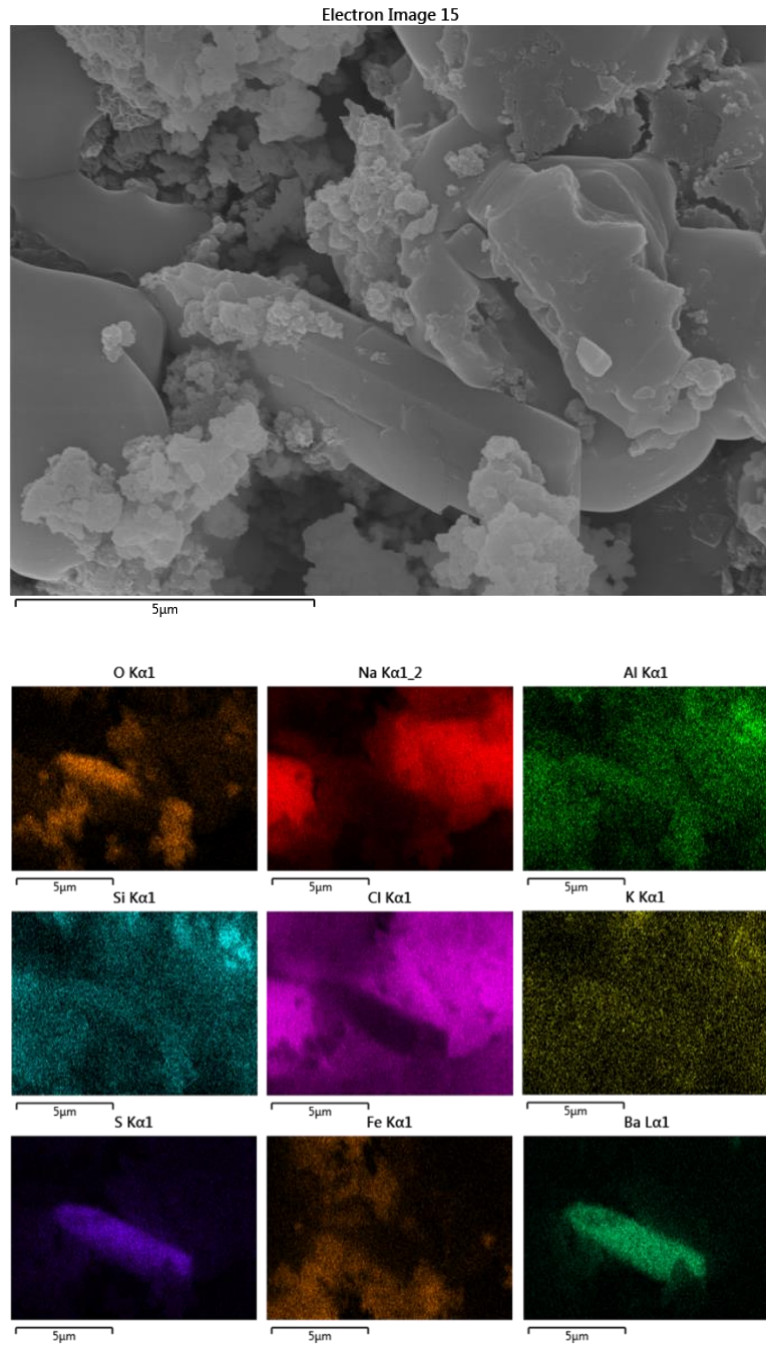
Figure 4.20 EDS mapping of geopolymer + medium 40% zeolite sample in 10,000 magnification.

Another aspect of a membrane's filtration performance is its ability to filter consistently for several cycles. Instead of repeated measurements of flow rate and water quality testing over several cycles when operated under constant pressure, testing water quality of filtered water under different pressures on the same membrane can also provide invaluable insight into long-term performance of the membranes. Recognizing that this was the first ever attempt to evaluate geopolymer composite membranes for filtering produced water, this approach was considered adequate for the present study. For this purpose, filtered water quality was compared for each data point shown in Figure 3.14 for each geopolymer composite membrane. Figure 4.21 shows optical images of the geopolymer+zeolite membrane with 40 vol% of fine zeolite after filtration studies were completed up to different pressures. Please note that these are images of the same membrane, which was subjected to filtration tests starting at 0.1 MPa for 10min, followed by subsequent studies conducted at higher pressures in steps of 0.1MPa. As can be seen, the quantity of particles retained on the membrane surface increased after each filtration step. Turbidity, TDS and pH values were presented in Table 4.9, the corresponding XRF analysis of the filtered water after each filtration study at different pressures are presented in Tables 4.12 through 4.15. The data shows that the filtration performance of each membrane remained invariant throughout.
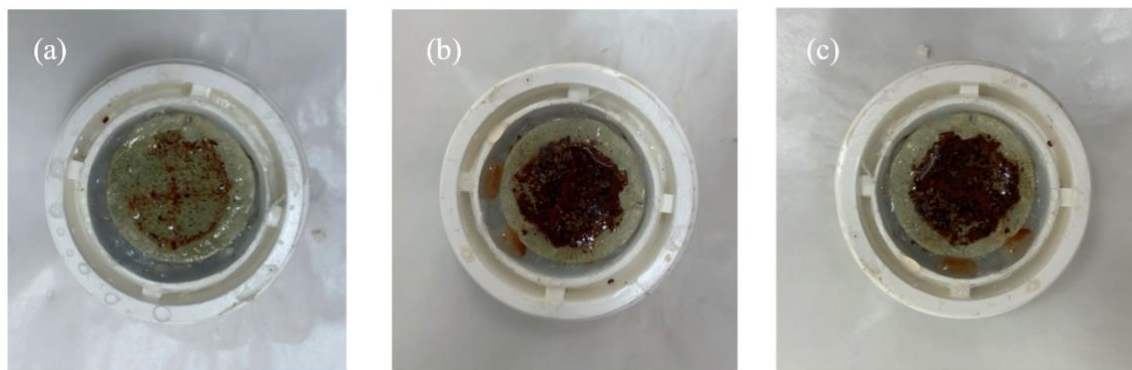
Figure 4.21 Photographs of a geopolymer+zeolite membrane with 40 vol% of fine zeolite after filtration studies conducted at (a) 0.1 MPa, (b) 0.5 MPa. (c) 0.9 MPa.

Table 4.12 XRF analysis of produced water filtered through geopolymer+zeolite (20 vol% of fine zeolite) composite membrane under different pressures. (unit: ppm)

Water Pressure	Cl	Na	Ca	Zn	Fe	Mg	Sr	P	S	Br	K	Si
0.1 MPa	169000	224000	20400	1670	56.6	2590	1160	4.90	32.6	792		
0.2 MPa	145000	95100	17200	622		2210	1180		31.3	844	805	46.7
0.3 MPa	147000	96500	18000	2170	63.8	2280	1000	4.02	21.1	747	740	50.4
0.4 MPa	172000	116000	20300	118		2670	1130		34.6	818	1080	62.8

Table 4.13 XRF analysis of produced water filtered through geopolymer+zeolite (40 vol% of fine zeolite) composite membrane under different pressures. (unit: ppm)

Water Pressure	Cl	Na	Ca	Zn	Fe	Mg	Sr	P	S	Br	K	Si
0.1 MPa	186000	114000	20900	18200	5220	2640	861	3.80	37.0	692	3010	74.1
0.2 MPa	168000	99800	20900	23300	2740	2660	1000		26.7	776	1090	30.9
0.3 MPa	183000	119000	20500	27500	3100	2360	942	2.58	36.0	715	745	24.6
0.4 MPa	179000	115000	20500	16600	1790	2520	985		31.8	731	586	41.7
0.5 MPa	179000	114000	21000	25000	3330	2490	1020	4.84	26.2	763	499	29.9
0.6 MPa	155000	88300	19400	17100	3870	2550	949		28.5	783	461	36.3
0.7 Mpa	136000	77400	17200	14100	5890	2270	907		28.8	706	374	34.6
0.8 Mpa	132000	61500	16600	23900	3230	2210	919		28.4	636	334	29.9

Table 4.14 XRF analysis of produced water filtered through geopolymer+zeolite (20 vol% of medium zeolite) composite membrane under different pressures. (unit: ppm)

Water Pressure	Cl	Na	Ca	Zn	Fe	Mg	Sr	P	S	Br	K	Si
0.1 MPa	141000	81800	18300	2660	60.0	2410	1020		27.4	791	4020	45.2
0.2 MPa	145000	89600	18000	3140	79.1	2440	1070	4.36	25.3	781	2240	57.6
0.3 MPa	145000	80900	19300	3130	168.0	2780	1010		31.9	763	1540	34.2
0.4 MPa	133000	74100	17700	2690	74.0	2550	1050		26.9	805	1110	43.1
0.5 MPa	138000	79000	17800	4830	79.7	2680	1030	1.50	24.9	813	971	33.5
0.6 MPa	128000	71700	16200	3800	57.7	2360	1000		23.2	681	850	32.3

Table 4.15 XRF analysis of produced water filtered through geopolymer+zeolite (40 vol% of medium zeolite) composite membrane under different pressures. (unit: ppm)

Water Pressure	Cl	Na	Ca	Zn	Fe	Mg	Sr	P	S	Br	K	Si
0.1 MPa	81600	26400	15900	1890	61.1	2290	969		27.6	701	1800	28.6
0.2 MPa	98300	41900	15800	4700	77.6	2250	1020		19.5	743		24.0
0.3 MPa	83800	28900	15200	3160	102.0	2220	978	3.67	17.4	676	755	30.3
0.4 MPa	93700	39000	15000	1880	62.0	2220	937		25.1	672	718	18.1

4.7 Summary

This study examined the potassium based geopolymer composition, processing conditions and two different types of additives to produce inexpensive geopolymer-based ceramic membranes for produced water filtration. The properties and performance of the developed membranes were analyzed for their microstructure, compressive strength, and filtration performance. Optimum composition for geopolymers for use in these applications was identified as $4SiO_2.Al_2O_3.11H_2O$, with best curing obtained at 60°C in 5 days.

Addition of biochar in excess of 6 vol% impeded the geopolymer phase formation. For smaller concentrations of biochar as an additive, the compressive strength reduced significantly. Insignificant reduction in impurity ion concentrations was observed when produced water was filtered through the geopolymer+biochar composite membranes. Therefore, it was concluded that geopolymer+biochar composite membranes are not suitable for filtration of produced water.

The results from the investigations on the geopolymer+zeolite composites were very promising. Geopolymer composites with fine or medium size particles of commercially available clinoptilolite could be processed as membranes for up to 40 vol% zeolite phase addition. Zeolite particles bonded well with the geopolymer matrix phase. Addition of zeolite phase can improve both the compressive strength and the filtration performance of geopolymer based ceramic membranes. The geopolymer+zeolite composite membrane sample with 40 vol% of fine zeolite particles showed a combination of high compressive strength, and flow rate. Although the most remarkable effect observed in water quality on filtration using these membranes was the decrease in turbidity, significant reduction in the concentrations of all ions except K was observed after filtration through the fine zeolite composite membranes. Overall, filtration performance of geopolymer composite membranes with fine zeolite was better than geopolymers with medium

zeolite. Preliminary studies also indicated that the filtration performance of the

geopolymer+zeolite membranes was invariant under different pressures.

CHAPTER V

GEOPOLYMER CAPSULES

5.1 Overview

The disposal routes such as landfilling and incineration, used for the disposal of solid waste, are

coming under increasing pressure due to restrict in land use and stringent environmental

legislations. Therefore, there is a need of an environmentally safe and cost-effective method for

the disposal or utilization of the solid waste for making valuable products. The immobilization of

the waste into a solid matrix is an attractive method for the disposal or recycling of the exhausted

adsorbent as the solidified adsorbent matrix could be disposed off in the landfill or recycled as a

construction material like bricks (Wang et al. 2015a, b). The purpose of this study was to assess

the use of geopolymeric materials to encapsulate waste generated from produced water treatment.

It is anticipated that the waste from produced water treatment could be in either of the following

two different forms (a) concentrated solutions of salts after filtration, or (b) powders of salts

obtained after evaporation of produced water. Encapsulation of both these two types of wastes

using geopolymers was evaluated in this study. For concentrated solution waste encapsulation,

the role of the geopolymeric phase as waste entrapment matrix was evaluated. On the other hand,

the solid waste, which is essentially crystallized water soluble salts present in produced water

along with all the inorganic contaminants, was "sealed" inside a cured geopolymer capsule. The ability of the geopolymeric phase to successfully contain the water soluble inorganic waste was evaluated by leaching studies in water.

5.2 Solid waste from produced water

As a first step it was important to understand the inorganic constituents present in produced water waste. For this purpose 500 ml of the produced water was evaporated to yield dried solid powder waste. The powder was ground and homogenized and analyzed by XRF. The results of XRF investigations on the solid waste are shown in the table 5.1.

Table 5.1 Elemental composition of the solid waste from produced water as analyzed by XRF (unit: ppm)

Na	Mg	Al	Si	P	S	Cl
194421	18484	56	166	1156	178	631692
K	**Ca**	**Fe**	**Br**	**Sr**	**Tl**	
2039	143991	427	3326	3956	108	

As expected, Na and Cl were the major constituents, with appreciable amounts of Ca and Mg besides other impurity elements.

5.3 Leaching test

The leaching studies were conducted following the standard method EA NEN 7375:2004. The purpose of this diffusion test is to determine the leaching of inorganic components from moulded and monolithic materials under aerobic conditions. Other parameters that can be deduced from the test include the extent of surface rinsing and the effective diffusion coefficient that can be used to estimate the leaching over longer periods. The test was performed on the cylindrical

samples with ~50.8 mm diameter and 21-28 mm height. The top view and side view of samples

for compressive test are shown in the Figure 5.1
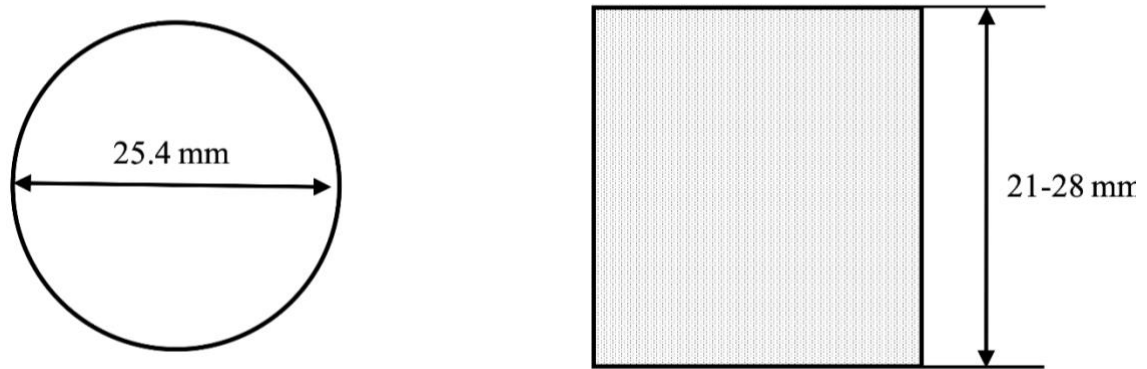
Figure 5.1 Top view and side view of the samples for leaching test

In this test a glass beaker with volume between two and five times the test piece volume (V_p) and

of dimensions such that the test piece was surrounded by at least 2 cm of water on all sides.

Demineralized water with a maximum conductivity of 1 µS/cm was used as the leaching medium.

This test was carried out in eight stages at room temperature, with temperature ranging between

18 and 22 °C. The glass beaker was rinsed with nitric acid, and subsequently with water before

performance of the test. Then the test piece was placed in the beaker, and the beaker was filled

with predetermined volume V of demineralized water such that $2 \times V_p \leqslant V \leqslant 5 \times V_p$. The

beaker was then covered to minimize evaporation while allowing for the stirrer paddle access into

the beaker (see Figure 5.2). Throughout these measurements the water was stirred at 60 rpm. The

first sampling of water quality was done after 6 ± 0.5 h, when the entire eluate was drained from

the beaker, and this is the fraction from period 1. The resulting eluate was tested for the pH ($\pm$

0.05), total conductivity, TDS, and turbidity, and precisely 200 µl was extracted from the eluate

for XRF testing. The remaining eluate was stored in plastic bottles for further testing, if required.

Immediately after drainage at the end of period 1, the beaker was refilled with the same quantity

81

V of water. The leaching test procedure described above was repeated for five more time periods as detailed in Table 5.2.

Figure 5.2 Experimental set up for leaching tests on geopolymer sample with encapsulated solid waste from produced water inside (left) and the control pure geopolymer sample (right).

Table 5.2 Times at which the water was sampled and replenished during the leaching studies.

Period (n)	Time (days)
1	$0.25 \pm 10\%$
2	$1 \pm 10\%$
3	$2.25 \pm 10\%$
4	$4 \pm 10\%$
5	$9 \pm 10\%$
6	$16 \pm 10\%$

5.4 Encapsulation in geopolymer matrix

To evaluate the use of geopolymer matrix to encapsulate the concentrated waste from produced water treatment, the waste solution itself was used to make geopolymer. The aim was to examine the possibility of using the geopolymer network to trap the ions in the produced water and prevent them from entering the environment by leaching. For this purpose, the following three samples were tested (a) Geopolymer prepared with 70% concentrated produced water (Gp-70), (b) Geopolymer with 80% concentrated produced water (Gp-80), and (c) Gp with 90% concentrated produced water (Gp-90).

5.4.1 Sample processing

Separate concentrated solutions were prepared by evaporating 500 ml of produced water to reduce the volume to 70 %, 80 % and 90 % for use in processing the Gp-70, Gp-80, and Gp-90 samples respectively. Same amount of concentrated produced water (approximately 35 ml) was used to make geopolymer samples. The process for making geopolymer with concentrated produced water is shown in the Figure 5.3 and the details of the three samples are shown in the Table 5.3.
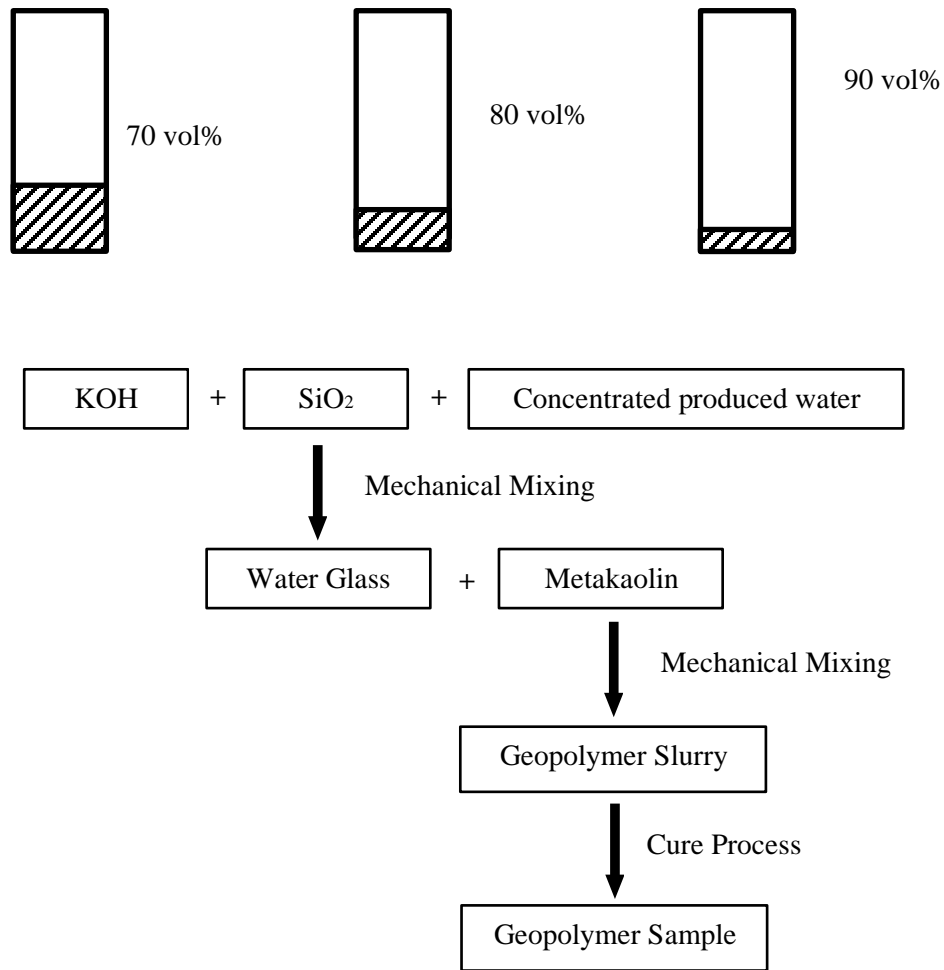
Figure 5.3 Schematic of the procedure followed for processing samples for geopolymer matrix encapsulation studies.

Table 5.3 Details of geopolymer samples prepared with concentrated produced water

Sample	Original amount of produced water (ml)	Concentrated amount of produced water (ml)
Gp-70	500.44	153.23
Gp-80	497.38	102.74
Gp-90	499.75	51.62

5.4.2 Leaching test results from geopolymer matrix encapsulation studies

The leaching tests were conducted for up to 16 days. Figure 5.4 and Table 5.4 shows the pH, TDS, turbidity and conductivity values for the leaching test. Four groups of sample were used for each leaching test, and pure geoplymer sample served as the benchmark or control.

As shown in Figure 5.4, very high TDS and conductivity values were measured at the onset of leaching, and gradually decreased to values coinciding with the control or the pure geopolymer sample. The turbidity values showed an initial spike during the testing period 1 (i.e. after 6 hours of leaching), and immediately subsided to values similar to the control sample. The TDS, conductivity and turbidity of the control samples were remarkably lower from the onset of the leaching experiment. The pH of all the sample solutions and the control sample started high, and gradually decreased. The trends observed in the TDS values measured for each sample could be explained by rapid leaching of all the ions present in the concentrated produced water used to prepare the samples. The low turbidity values reported in these studies just reaffirm that no insoluble particulate matter was released to the water, and only soluble species were leached out. The trends in the pH can be explained on the basis of unreacted KOH from the

Table 5.4 pH, TDS, Turbidity and Conductivity results of leached water

Time (Days)	Sample Group	pH	TDS (ppm)	Conductivity (µS)	Turbidity (NTU)
0.25	Control	10.928	338	660	0.7
	Gp-70	11.164	2160	4500	0.14
	Gp-80	11.832	5270	10800	2.59
	Gp-90	11.664	6270	13440	2.41
1	Control	10.715	225	463	0.14
	Gp-70	11.137	1220	2510	0.25
	Gp-80	11.735	2700	5050	0.4
	Gp-90	11.629	3400	7040	0.91
2.25	Control	10.087	163	337	0.06
	Gp-70	10.688	511	1066	0.14
	Gp-80	11.375	1200	2520	0.3
	Gp-90	11.175	1340	2760	0.75
4	Control	9.851	128	266	0.02
	Gp-70	10.471	304	633	0.27
	Gp-80	10.917	596	1236	0.19
	Gp-90	10.783	656	1359	0.24
9	Control	9.349	182	379	0.07
	Gp-70	10.021	362	753	0.11
	Gp-80	10.206	530	1105	0.89
	Gp-90	10.197	587	1217	0.35
16	Control	8.825	136	285	0.10
	Gp-70	9.517	252	523	0.11
	Gp-80	9.925	322	666	0.08
	Gp-90	9.940	360	750	0.39
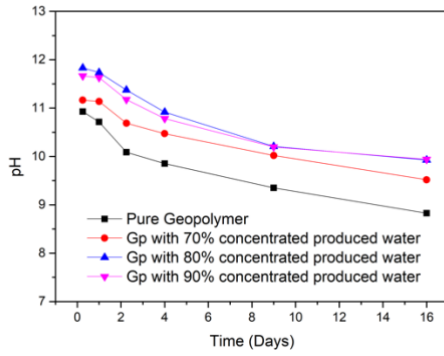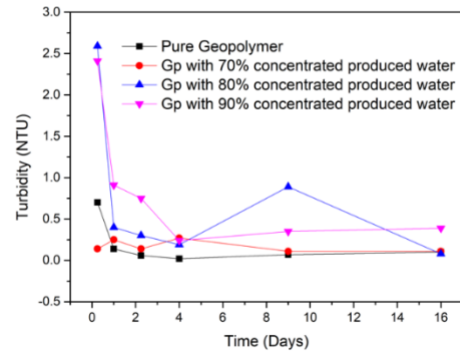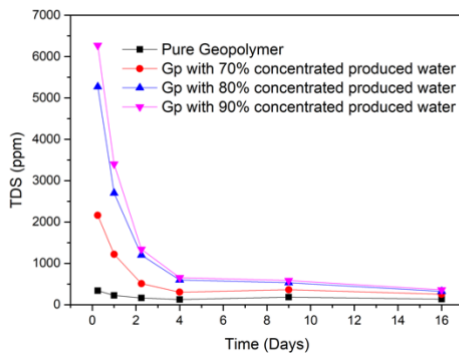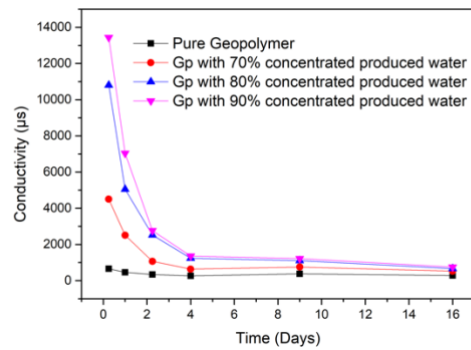
Figure 5.4 pH, turbidity, TDS and conductivity plots from the leaching studies conducted to evaluate the feasibility of concentrated waste encapsulation in the geopolymer matrix.

geopolymer matrix, with potentially more unreacted KOH available for leaching from the Gp-70, Gp-80 and the Gp-90 samples. These studies lead to the conclusion that although geopolymers could be processed and cured using the concentrate waste from produced water treatment, the geopolymer network is unable to trap the water soluble ions in the produced water and prevent them from entering the environment by leaching.

5.5 Geopolymer capsule

The purpose of this part of the study was to evaluate the use of geopolymers to fabricate a dense capsule enclose the solid waste from produced water evaporation, to prevent it from leaching to

the environment. Geopolymers are porous, but they lack permeability. This property of the geopolymer was the primary factor that motivated this part of the study. Details on the processing of the capsule, encapsulation of the solid waste, and subsequent evaluation of leaching properties are presented in the following sections.

5.5.1 Processing of geopolymer capsule

A two step process was followed to make the geopolymer capsule. In the first step, a cylindrical geopolymer mold with a cylindrical cavity was processed. Once cured, approximately 9.15 g of solid waste from produced water evaporation was placed inside the cavity. In the second step, the cavity was sealed with geopolymer slurry (after placing a geopolymer spacer above the solid waste), and allowed to cure to process the capsule. The procedure followed for making the geopolymer capsule is shown in the Figure 5.5.

Figure 5.5 Schematic diagram of the process followed for making geopolymer capsule samples
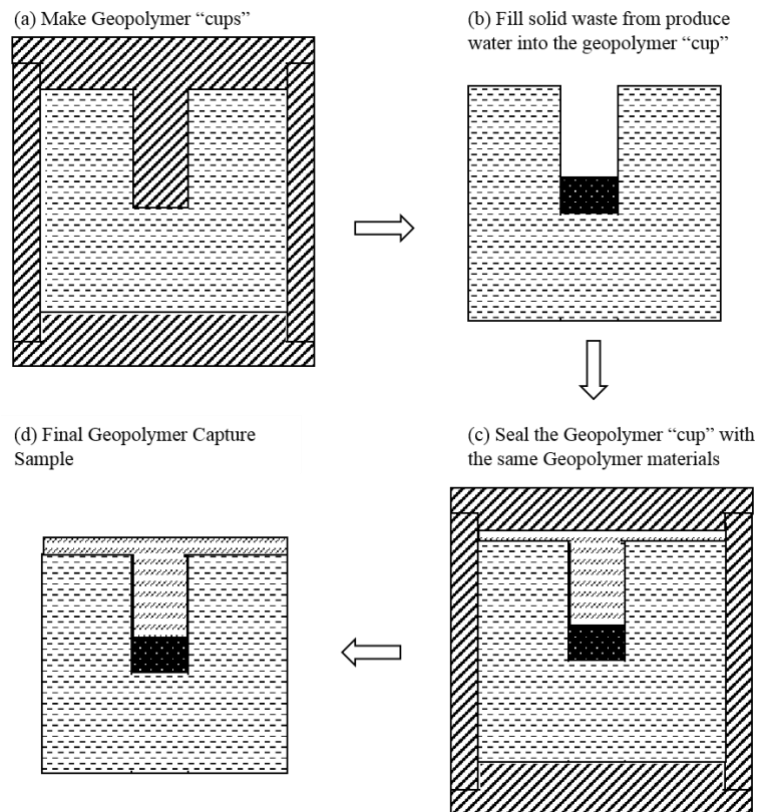
5.5.2 Leaching test result of geopolymer capsule

Two groups of sample were been use for leaching test. First group is the geopolymer capsule with the solid waste inside it (Sample group), the other group is pure geopolymer in the same size with sample group (Control group).The leaching tests were conducted for up to 9 days following the same procedures as outlined in section 5.3. Table 5.5 shows the pH, TDS, turbidity and conductivity values for the leaching tests after 6 hours, 1 day, 2.25 days, 4 days and 9 days. Figure 5.6 is graphical representation of the data presented in Table 5.5 to assist with visual observation of any trends.

Table 5.5 pH, TDS, Turbidity and Conductivity results of leaching water

Time (Days)	Sample Group	pH	TDS (ppm)	Conductivity (µS)	Turbidity (NTU)
Produced Water		4.120	55100	184500	77.7
0.25	Sample	9.649	1190	2420	0.15
	Control	10.764	621	1269	0.05
1	Sample	8.421	840	2960	0.07
	Control	10.689	396	1338	0
2.25	Sample	8.470	860	2940	0.05
	Control	10.512	229	778	0.08
4	Sample	8.452	1020	3450	0.06
	Control	10.378	153	520	0.04
9	Sample	7.975	1840	6170	0.04
	Control	10.163	168	608	0.14

As shown in Figure 5.6, TDS and conductivity values for the sample group was only marginally higher than the control group at the onset of leaching. However, with time, these values gradually increased in contrast to the pure geopolymer samples which decreased over the same time period. The turbidity values were remarkably low for both the sample and control group samples. The pH of all the sample group and the control sample started high, and gradually decreased. The trends
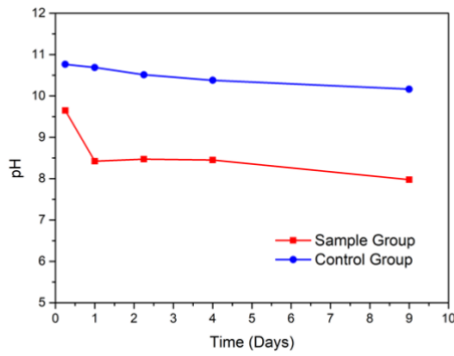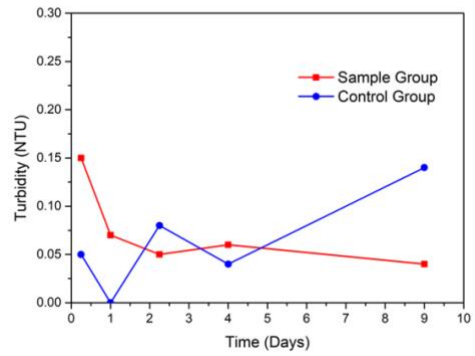
(a)   (b)
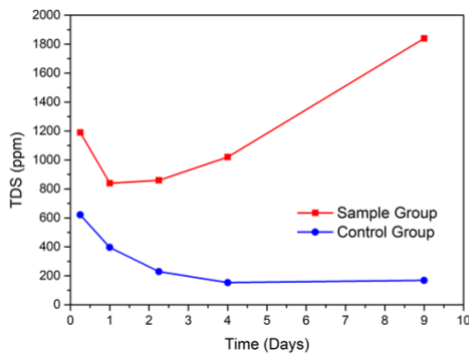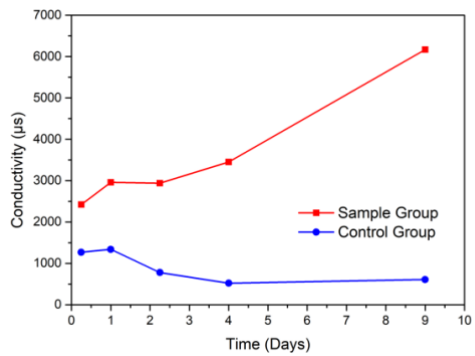
(c)   (d)

Figure 5.6 pH, turbidity, TDS and conductivity plots from the leaching studies conducted to evaluate the feasibility of solid waste encapsulation in the geopolymer capsule.

observed in the TDS and conductivity values measured for the sample group could be explained by dissolution followed by slow leaching of the elements present in the solid waste from the produced water secured inside the geopolymer capsule. The trends in the pH can be explained on the basis of unreacted KOH from the geopolymer matrix. Interestingly the pH of the eluate in the control group studies was higher than the sample group. These studies are quite preliminary, however they do highlight the potential of geopolymer capsules to arrest water soluble wastes. Further investigations in this direction should focus on optimization of pure geopolymer compositions, and certainly leaching studies over a longer duration of time.

5.6 Summary

This study successfully evaluated the use of geopolymeric materials to encapsulate waste generated from produced water treatment. Encapsulation of two different forms of waste from produced water treatment that was investigated included, (a) concentrated solutions of salts after filtration, and (b) powders of salts obtained after evaporation of produced water. For concentrated solution waste encapsulation, the geopolymeric phase itself was used to entrap the impurity ions. The solid waste, on the other hand, was "sealed" inside a cured geopolymer capsule. The ability of the geopolymers to successfully contain these water soluble inorganic waste forms was evaluated by leaching studies in water.

The key findings of this study were that although geopolymers could be processed and cured using the concentrate waste from produced water treatment, the geopolymer network is unable to trap the water soluble impurity ions and prevent them from entering the environment by leaching. On the other hand, the studies conducted to evaluate the use of geopolymer capsules to contain solid waste forms from produced water evaporation were quite encouraging. Geopolymer capsules do hold promise as encapsulating containers to restrain water soluble salts from leaching into the environment. However, these studies were preliminary, and further investigations are required to establish this.

CHAPTER VI

CONCLUSIONS AND FUTURE WORK

This research investigated the use of inexpensive metakaolin based potassium geopolymers for produced water treatment. Towards this goal two different research directions were pursued. The focus of the first research thrust was to develop and evaluate the use of geopolymer based ceramic composite membranes for filtration of produced water. The second effort examined the feasibility of the use of geopolymers to encapsulate the waste resulting from produced treatment. Entrapment of two different types of waste, specifically concentrated solutions from produced water and solid waste resulting from evaporating produced water, was investigated. The findings of this research are summarized in the following sections, and suggestions are also provided to serve as guidelines for future work.

6.1 Conclusions

6.1.1 Geopolymeric ceramic membranes:

The key findings of this research thrust are:

- The optimum composition of geopolymers to develop composite membranes was identified as $4SiO_2.Al_2O_3.11H_2O$. For this composition, best curing occurred at 60°C in 5 days.

- Biochar was not a suitable additive for geoplymers to process ceramic composite membranes. The geopolymer+biochar composites had reduced compressive strength, and

- the membranes showed poor filtration performance.

- Natural zeolite (clinoptilolite) addition to geopolymers holds considerable promise to develop ceramic composite membranes for produced water treatment. Zeolite particles bonded well with the geopolymer matrix phase. Addition of zeolite phase can improve both the compressive strength and the filtration performance of geopolymer based ceramic membranes. Filtration using these composite membranes not only decreased the turbidity, but significant reduction in the concentrations of all ions except K was also observed. Overall, filtration performance of geopolymer+zeolite composite membranes improved with decrease in particle size of the zeolite.

6.1.2 Waste encapsulation using geopolymers

The key findings of this research thrust are:

- Geopolymers can be successfully processed and cured using the concentrate waste from produced water treatment, however the geopolymer network is unable to trap the water soluble impurity ions and prevent them from entering the environment by leaching.

- Geopolymer capsules do hold promise as encapsulating containers to restrain water soluble salts from leaching into the environment. However, these studies were preliminary, and further investigations are required to establish this.

6.2 Future work

This research was the first-ever systematic effort to explore the use of geopolymers for the development of ceramic membranes for produced water treatment, and for encapsulation of resulting waste. Promising directions for future work as well as some limitations that may need to be addressed for development of this application are presented below:

- Optimization of the concentration of fine zeolite powders in geopolymer+zeolite

membranes should be explored to produce microstructures that can enable even nanofiltration capabilities.

- Design and development of porous scaffolds that can support thin (<100 micron) ceramic composite membranes should be pursued to enable much higher flux.

- Experimental set-up should be developed to test these membranes in cross-filtration mode.

- The procedure for the use of XRF to determine the water quality should be standardized. This is particularly important for the analysis of solutions which have suspended particles as well as dissolved ions.

- Geopolymeric waste encapsulation containers holds considerable promise. The flexibility in composition to form geopolymeric phase, can be an advantage in designing containers for low grade radioactive waste.

REFERENCES

Alpatova, A., Kim, E.-S., Dong, S., Sun, N., Chelme-Ayala, P., and Gamal El-Din, M., 2014, Treatment of oil sands process-affected water with ceramic ultrafiltration membrane: Effects of operating conditions on membrane performance: Separation and Purification Technology, v. 122, p. 170-182.

Aysu, T., and Küçük, M. M., 2014, Biomass pyrolysis in a fixed-bed reactor: Effects of pyrolysis parameters on product yields and characterization of products: Energy, v. 64, p. 1002-1025.

Bader, M. S. H., 2007, Seawater versus produced water in oil-fields water injection operations: Desalination, v. 208, no. 1, p. 159-168.

Bai, C., Franchin, G., Elsayed, H., Zaggia, A., Conte, L., Li, H., and Colombo, P., 2017, High-porosity geopolymer foams with tailored porosity for thermal insulation and wastewater treatment: Journal of Materials Research, v. 32, no. 17, p. 3251-3259.

Bakharev, T., 2005, Resistance of geopolymer materials to acid attack: Cement and concrete research, v. 35, no. 4, p. 658-670.

Bao, Y., Grutzeck, M. W., and Jantzen, C., 2005, Preparation and Properties of Hydroceramic Waste Forms Made With Simulated Hanford Low-Activity Waste: Journal of the American Ceramic Society, v. 88, p. 3287-3302.

Barukčić, I., Božanić, R., and Kulozik, U., 2014, Effect of pore size and process temperature on flux, microbial reduction and fouling mechanisms during sweet whey cross-flow microfiltration by ceramic membranes: International Dairy Journal, v. 39, no. 1, p. 8-15.

Benko, K. L., and Drewes, J. E., 2008, Produced water in the Western United States: geographical distribution, occurrence, and composition: Environmental Engineering Science, v. 25, no. 2, p. 239-246.

Bhutta, M. A. R., Ariffin, N. F., Hussin, M. W., and Lim, N. H. A. S., 2013, Sulfate and sulfuric acid resistance of geopolymer mortars using waste blended ash: Jurnal teknologi, v. 61, no. 3.

Bhutta, M. A. R., Hussin, W. M., Azreen, M., and Tahir, M. M., 2014, Sulphate resistance of geopolymer concrete prepared from blended waste fuel ash: Journal of Materials in Civil Engineering, v. 26, no. 11, p. 04014080.

Bilstad, T., and Espedal, E., 1996, Membrane separation of produced water: Water Science and Technology, v. 34, no. 9, p. 239-246.

Blanchard, E., 2013, Oil in water monitoring is a key to production separation: EOR, mature fields push discharge amounts higher: Offshore, v. 73, no. 11.

Bridgwater, A., Toft, A., and Brammer, J., 2002, A techno-economic comparison of power production by biomass fast pyrolysis with gasification and combustion: Renewable and Sustainable Energy Reviews, v. 6, no. 3, p. 181-246.

Castel, A., and Foster, S. J., 2015, Bond strength between blended slag and Class F fly ash geopolymer concrete with steel reinforcement: Cement and Concrete Research, v. 72, p. 48-53.

Chen, A. S. C., Flynn, J. T., Cook, R. G., and Casaday, A. L., 1991, Removal of Oil, Grease, and Suspended Solids From Produced Water With Ceramic Crossflow Microfiltration: SPE Production Engineering, v. 6, no. 02, p. 131-136.

Cheryan, M., and Rajagopalan, N., 1998, Membrane processing of oily streams. Wastewater treatment and waste reduction: Journal of Membrane Science, v. 151, no. 1, p. 13-28.

Ciarapica, F., and Giacchetta, G., 2003, The Treatment of "Produced Water" in Offshore Rig: Comparison Between Traditional Installations and Innovative Systems.

Cronstedt, A. F., Schlenker, J. L., and Kühl, G. H., Observations and Descriptions: On an Unknown Mineral-Species Called Zeolites, *in* Proceedings Proceedings from the Ninth International Zeolite Conference1993, Elsevier, p. 3-9.

Davidovits, J., 1989, Geopolymers and geopolymeric materials: Journal of Thermal Analysis and Calorimetry, v. 35, no. 2, p. 429-441.

Davidovits, J., 2008, Geopolymer Chemistry and Applications.

Deriszadeh, A., Husein, M. M., and Harding, T. G., 2010, Produced Water Treatment by Micellar-Enhanced Ultrafiltration: Environmental Science & Technology, v. 44, no. 5, p. 1767-1772.

Duxson, P., Provis, J. L., Lukey, G. C., Mallicoat, S. W., Kriven, W. M., and van Deventer, J. S. J., 2005, Understanding the relationship between geopolymer composition, microstructure and mechanical properties: Colloids and Surfaces A: Physicochemical and Engineering Aspects, v. 269, no. 1-3, p. 47-58.

Duxson, P., Provis, J. L., Lukey, G. C., and van Deventer, J. S. J., 2007, The role of inorganic polymer technology in the development of 'green concrete': Cement and Concrete Research, v. 37, no. 12, p. 1590-1597.

Emani, S., Uppaluri, R., and Purkait, M. K., 2014, Microfiltration of oil–water emulsions using low cost ceramic membranes prepared with the uniaxial dry compaction method: Ceramics International, v. 40, no. 1, Part A, p. 1155-1164.

Fakhru'l-Razi, A., Pendashteh, A., Abdullah, L. C., Biak, D. R. A., Madaeni, S. S., and Abidin, Z. Z., 2009, Review of technologies for oil and gas produced water treatment: Journal of hazardous materials, v. 170, no. 2-3, p. 530-551.

Fernández-Jiménez, A., Palomo, A., Sobrados, I., and Sanz, J., 2006, The role played by the reactive alumina content in the alkaline activation of fly ashes: Microporous and Mesoporous Materials, v. 91, no. 1, p. 111-119.

Gartner, E., 2004, Industrially interesting approaches to "low-CO2" cements: Cement and Concrete Research, v. 34, no. 9, p. 1489-1498.

Gaunt, J. L., and Lehmann, J., 2008, Energy Balance and Emissions Associated with Biochar Sequestration and Pyrolysis Bioenergy Production: Environmental Science & Technology, v. 42, no. 11, p. 4152-4158.

Georgie, W. J., 2002, Effective and Holistic Approach to produced Water Management for Offshore Operation, Offshore Technology Conference: Houston, Texas, Offshore Technology Conference, p. 13.

Glaser, B., Lehmann, J., and Zech, W., 2002, Ameliorating physical and chemical properties of highly weathered soils in the tropics with charcoal–a review: Biology and fertility of soils, v. 35, no. 4, p. 219-230.

Hansen, B., and Davies, S., 1994, Review of potential technologies for the removal of dissolved components from produced water: Chemical engineering research & design, v. 72, no. 2, p. 176-188.

He, P., Jia, D., Lin, T., Wang, M., and Zhou, Y., 2010, Effects of high-temperature heat treatment on the mechanical properties of unidirectional carbon fiber reinforced geopolymer composites: Ceramics International, v. 36, no. 4, p. 1447-1453.

Judd, S., 2010, The MBR Book: Principles and Applications of Membrane Bioreactors for Water and Wastewater Treatment, Elsevier Science.

Kambo, H. S., and Dutta, A., 2015, A comparative review of biochar and hydrochar in terms of production, physico-chemical properties and applications: Renewable and Sustainable Energy Reviews, v. 45, p. 359-378.

Khulbe, K. C., Feng, C., and Matsuura, T., 2010, The art of surface modification of synthetic polymeric membranes: Journal of Applied Polymer Science, v. 115, no. 2, p. 855-895.

Korkuna, O., Leboda, R., Skubiszewska-Zie, b. J., Vrublevs'Ka, T., Gun'Ko, V., and Ryczkowski, J., 2006, Structural and physicochemical properties of natural zeolites: clinoptilolite and mordenite: Microporous and Mesoporous Materials, v. 87, no. 3, p. 243-254.

Krivenko, P., and Kovalchuk, G. Y., 2007, Directed synthesis of alkaline aluminosilicate minerals in a geocement matrix: Journal of Materials Science, v. 42, no. 9, p. 2944-2952.

Lalia, B. S., Kochkodan, V., Hashaikeh, R., and Hilal, N., 2013, A review on membrane fabrication: Structure, properties and performance relationship: Desalination, v. 326, p. 77-95.

Lee, J. M., and Frankiewicz, T. C., 2005, Treatment of Produced Water with an Ultrafiltration (UF) Membrane-A Field Trial, SPE Annual Technical Conference and Exhibition: Dallas, Texas, Society of Petroleum Engineers, p. 6.

Li, Y. S., Yan, L., Xiang, C. B., and Hong, L. J., 2006, Treatment of oily wastewater by organic–inorganic composite tubular ultrafiltration (UF) membranes: Desalination, v. 196, no. 1, p. 76-83.

Lord, P. D., and LeBas, R., 2013, Treatment Enables High-TDS Water Use as Base Fluid for Hydraulic Fracturing: Journal of Petroleum Technology, v. 65, no. 06, p. 30-33.

Mallicoat, S., Sarin, P., and Kriven, W. M., 2005, Novel, alkali-bonded, ceramic filtration membranes, *in* Brito, M. E., Filip, P., Lewinsohn, C., Sayir, A., Opeka, M., and Mullins, W. M., eds., 29th Internationa Conference on Advanced Ceramics and Composites: Cocoa Beach, FL, The American Ceramic Society.

Marakatti, V. S., Rao, P. V.C., Choudary, N. V., Ganesh, G. S., Shah, G., Maradur, S. P., Halgeri, A. B., Shanbhag, G. V. and Ravishankar, R., 2015a, Influence of Alkaline Earth Cation Exchanged X-Zeolites Towards Ortho-Selectivity in Alkylation of Aromatics: Hard-Soft-Acid-Base Concept: Advanced Porous Materials, v. 2, no. 4, p. 221-229.

Marakatti, V. S., 2015b, Metal ion-exchanged zeolites as highly active solid acid catalysts for the green synthesis of glycerol carbonate from glycerol: RSC Advances, v. 5, p. 14286-14293

Murić, A., Petrinić, I., and Christensen, M. L., 2014, Comparison of ceramic and polymeric ultrafiltration membranes for treating wastewater from metalworking industry: Chemical Engineering Journal, v. 255, p. 403-410.

Neff, J., Sauer, T., and Maciolek, N., 1992, Composition, Fate and Effects of Produced Water
Discharges to Nearshore Marine Waters, p. 371-385.

Nikolov, A., Rostovsky, I., and Nugteren, H., 2017, Geopolymer materials based on natural
zeolite: Case studies in construction materials, v. 6, p. 198-205.

Oklahoma-PWWG, 2017, Oklahoma Water for 2060 Produced Water Reuse and Recycling:
OWRB.

OWRB, 2012, Update of the Oklahoma Comprehensive Water Plan.

Palomo, A., and López dela Fuente, J. I., 2003, Alkali-activated cementitous materials:
Alternative matrices for the immobilisation of hazardous wastes: Part I. Stabilisation of
boron: Cement and Concrete Research, v. 33, no. 2, p. 281-288.

Rahier, H., Mele, B., Biesemans, M., Wastiels, J., and Wu, X., 1996, Low-temperature
synthesized aluminosilicate glasses: Journal of Materials Science, v. 31, p. 71-79.

Škvára, F., Alkali activated material–geopolymer, *in* Proceedings International Conference Alkali
Activated Materials–Research, Production and Utilization, Česká rozvojová agentura,
Praha2007, p. 21-22.26.

Sofi, M., Deventer, J. S. J., Mendis, P. A., and Lukey, G. C., 2007, Bond performance of
reinforcing bars in inorganic polymer concrete (IPC): Journal of Materials Science, v. 42,
p. 3107-3116.

Sonune, A., and Ghate, R., 2004, Developments in wastewater treatment methods: Desalination,
v. 167, p. 55-63.

Stephenson, M. T., 1992, A Survey of Produced Water Studies, *in* Ray, J. P., and Engelhardt, F. R., eds., Produced Water: Technological/Environmental Issues and Solutions: Boston, MA, Springer US, p. 1-11.

Swaddle, T. W., 2001, Silicate complexes of aluminum(III) in aqueous systems: Coordination Chemistry Reviews, v. 219-221, p. 665-686.

Swaddle, T. W., Salerno, J., and Tregloan, P. A., 1994, Aqueous aluminates, silicates, and aluminosilicates: Chemical Society Reviews, v. 23, no. 5, p. 319-325.

Szép, A., and Kohlheb, R., 2010, Water treatment technology for produced water: Water Science and Technology, v. 62, no. 10, p. 2372-2380.

Temuujin, J., Minjigmaa, A., Rickard, W., Lee, M., Williams, I., and Van Riessen, A., 2009, Preparation of metakaolin based geopolymer coatings on metal substrates as thermal barriers: Applied clay science, v. 46, no. 3, p. 265-270.

Thokchom, S., Ghosh, P., and Ghosh, S., 2009, Acid resistance of fly ash based geopolymer mortars: International Journal of Recent Trends in Engineering, v. 1, no. 6, p. 36.

Tripathi, M., Sahu, J. N., and Ganesan, P., 2016, Effect of process parameters on production of biochar from biomass waste through pyrolysis: A review: Renewable and Sustainable Energy Reviews, v. 55, p. 467-481.

van Jaarsveld, J., and Van Deventer, J., 1999, Effect of the alkali metal activator on the properties of fly ash-based geopolymers: Industrial & engineering chemistry research, v. 38, no. 10, p. 3932-3941.

Veil, J. A., 2011, Produced Water Management Options and Technologies, *in* Lee, K., and Neff, J., eds., Produced Water: Environmental Risks and Advances in Mitigation Technologies: New York, NY, Springer New York, p. 537-571.

Veil, J. A., Puder, M. G., Elcock, D., and Redweik, R. J., Jr., 2004, A white paper describing produced water from production of crude oil, natural gas, and coal bed methane.

Winsley, P., 2007, Biochar and bioenergy production for climate change mitigation: New Zealand Science Review Vol, v. 64.

Xu, P., Drewes, J. E., and Heil, D., 2008, Beneficial use of co-produced water through membrane treatment: technical-economic assessment: Desalination, v. 225, no. 1, p. 139-155.

Zeidler, S., Puhlfürß, P., Kätzel, U., and Voigt, I., 2014, Preparation and characterization of new low MWCO ceramic nanofiltration membranes for organic solvents: Journal of Membrane Science, v. 470, p. 421-430.

VITA

Ying Xu

Candidate for the Degree of

Master of Science

Thesis: STUDIES ON THE USE OF METAKAOLIN GEOPOLYMER FOR PRODUCED WATER TREATMENT

Major Field: Material Science and Engineering

Biographical:

Education:

Completed the requirements for the Master of Science in Materials Science and Engineering at Oklahoma State University, Tulsa, Oklahoma in December, 2019.

Completed the requirements for the Bachelor of Engineering in Metallurgical Engineering at University of Science and Technology Beijing, Beijing, China in 2015.

Experience:
Teaching Assistant, Oklahoma State University, Stillwater, Oklahoma (2018-2019)

Professional Memberships:
Member, American Ceramic Society
Member, American Chemical Society